The Physics of Gamma-Ray Bursts

Bing Zhang

University of Nevada Las Vegas

Jul. 11, 2019

HEPRO-VII
Barcelona, Jul. 9-12, 2019

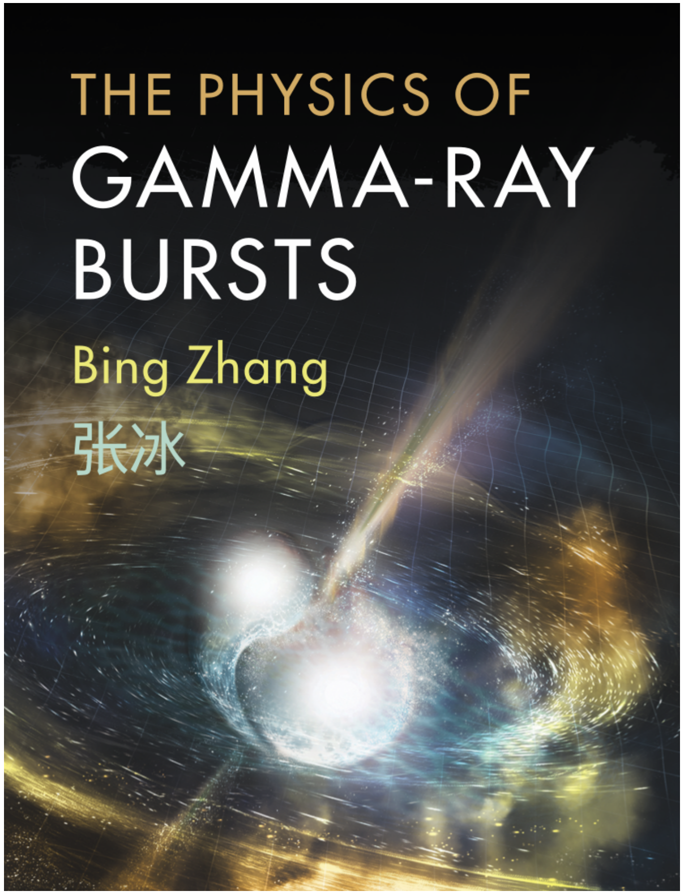

Open Questions in GRB Physics

- Ejecta composition (fireball vs. Poynting jet vs. hybrid)
- Energy dissipation mechanism (shock vs. magnetic reconnection)
- Particle acceleration & radiation mechanisms (synchrotron, inverse Compton, quasi-thermal Comptonization)
- Progenitors & classification (massive stars vs. compact stars)
- Central engine (black hole vs. magnetar)
- Geometry (uniform jet vs. structured jet; jet vs. cocoon)
- Afterglow physics (medium interaction vs. long-term engine activity)

Prompt GRB Emission:
a Mystery

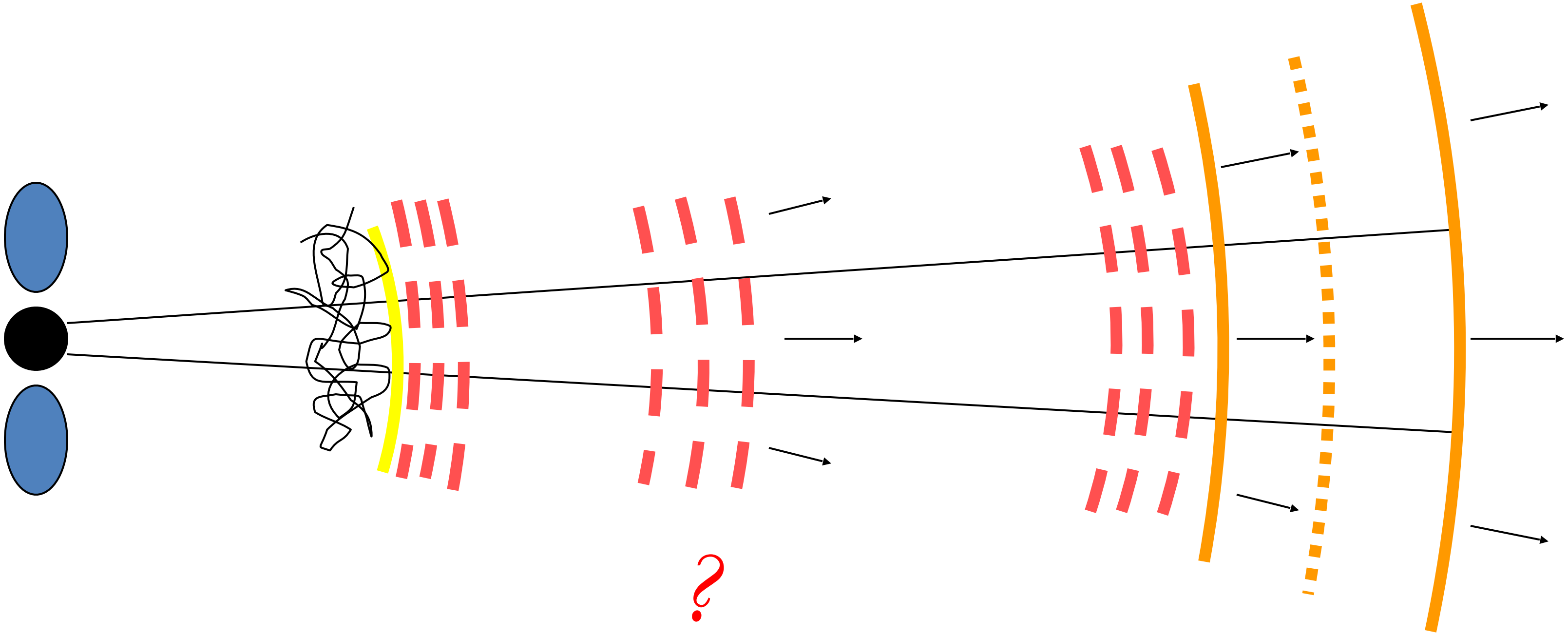

central engine

photosphere

internal

external shocks

(reverse)

(forward)

What is the jet composition (baryonic vs. Poynting flux)?

Where is (are) the dissipation radius (radii)?

How is the radiation generated (synchrotron, Compton scattering, thermal)?

What?

Jet Composition (matter vs. magnetic)

Energy dissipation (shock vs. reconnection)

Early GRB model:
The fireball shock model

(Paczynski, Meszaros, Rees, Piran, Sari, …)

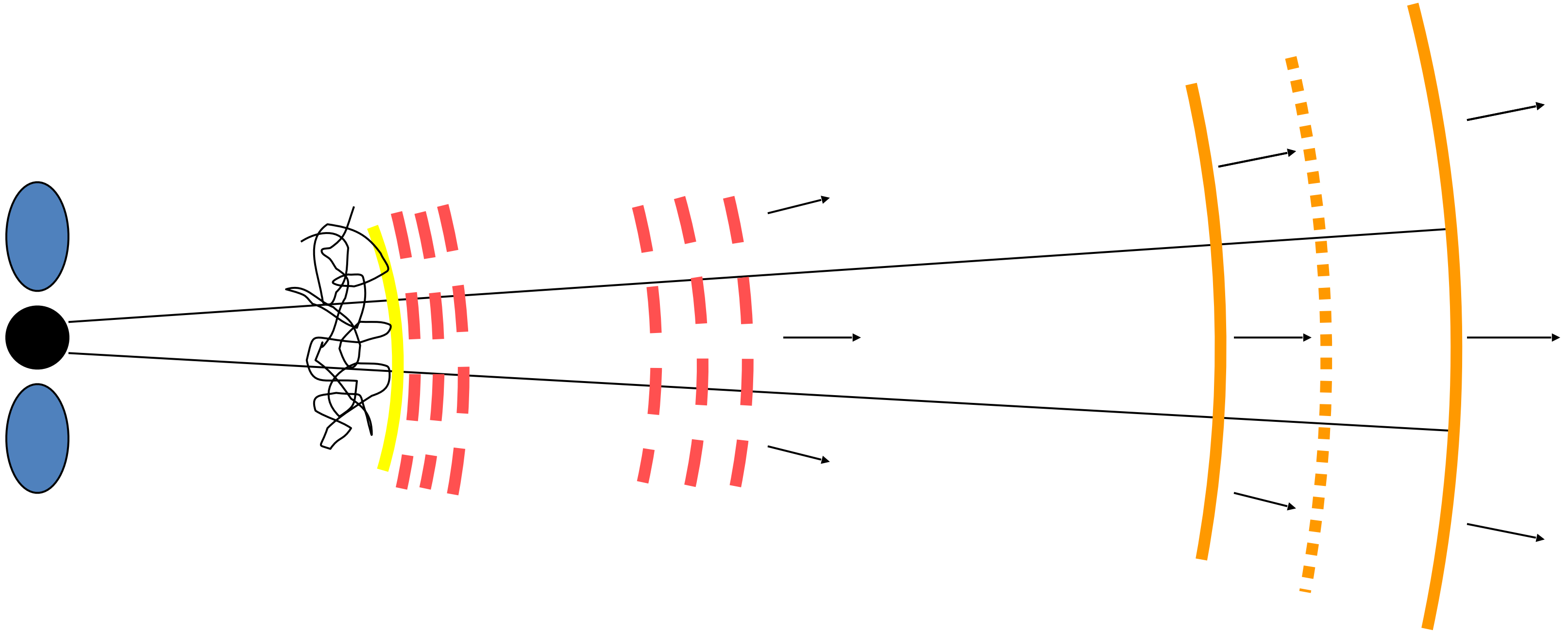

central engine

photosphere

internal

external shocks

(reverse) ***(forward)***

Before Fermi: Fireball Predictions:
Internal shock synchrotron vs. photosphere

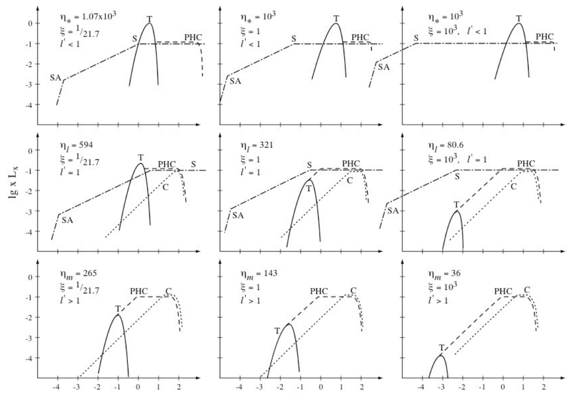

Meszaros & Rees (00)

1276 *F. Daigne and R. Mochkovitch*

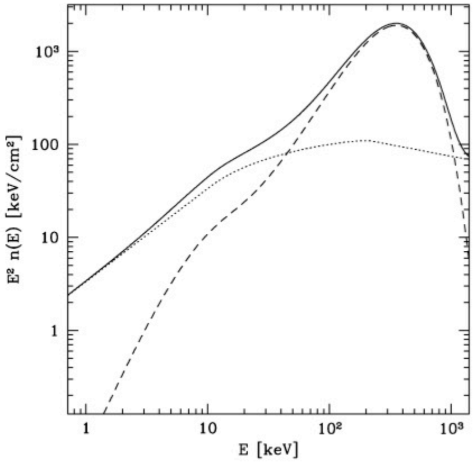

Daigne & Mochkovitch (02)

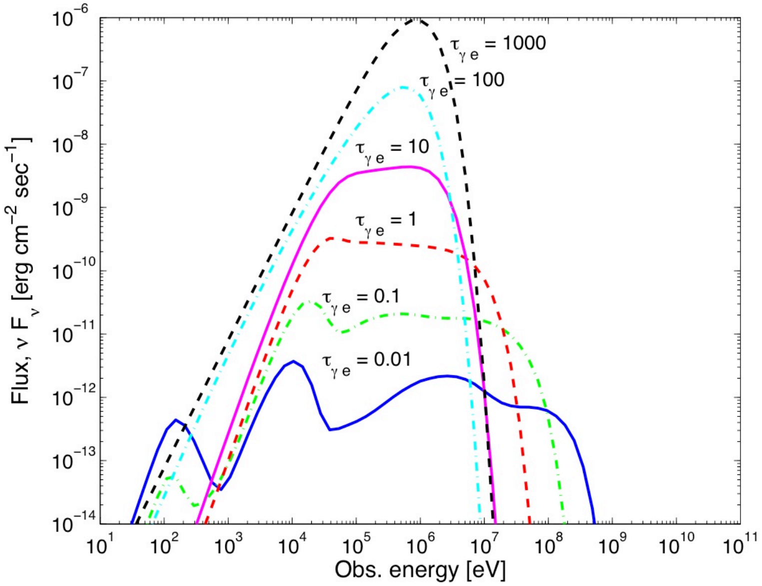

Pe'er et al. (06)

Fermi: a much wider spectral window

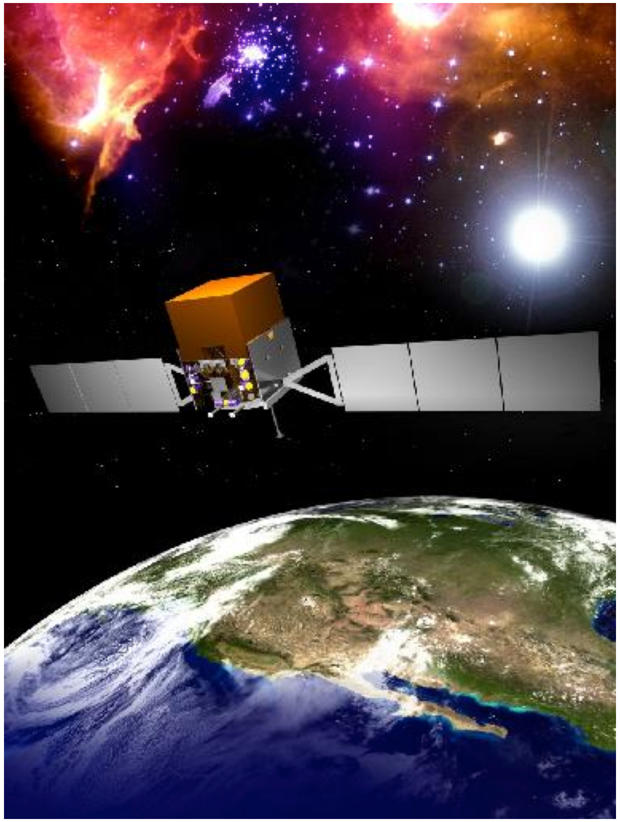

Launched on June 11th, 2008

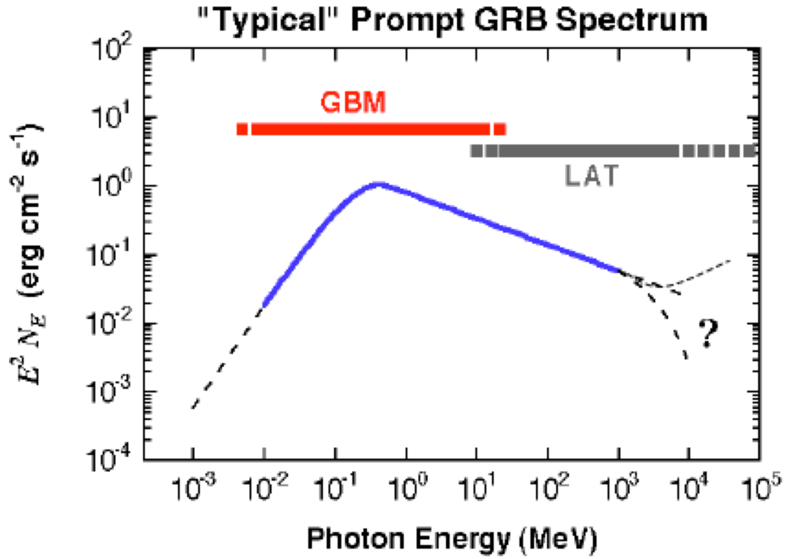

Fermi surprise: GRB 080916C

(Abdo et al. 2009, Science)

$z = 4.35 \pm 0.15$

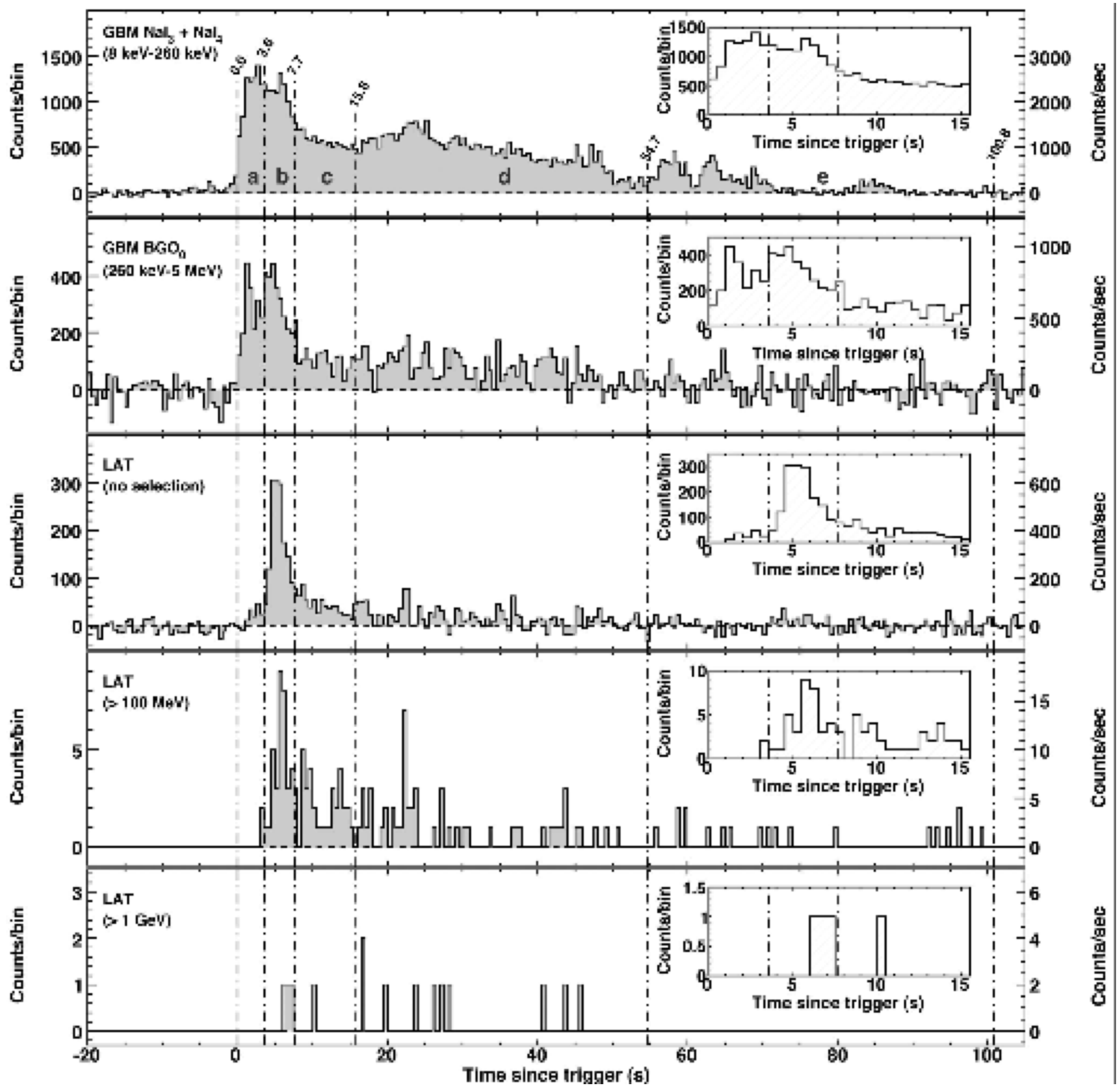

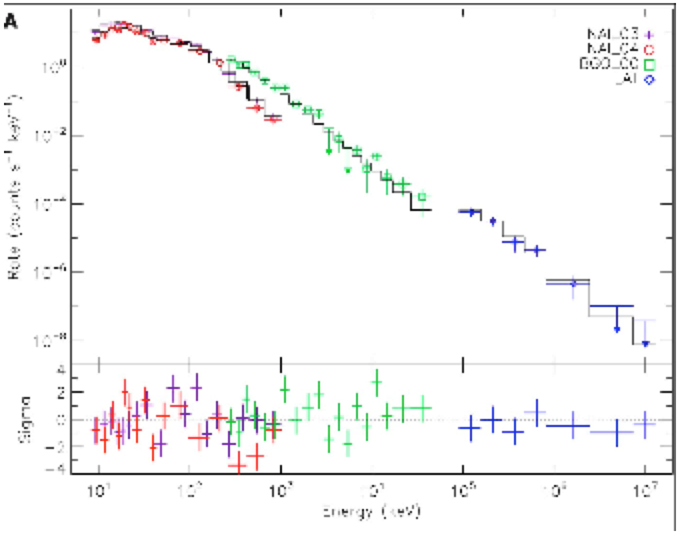

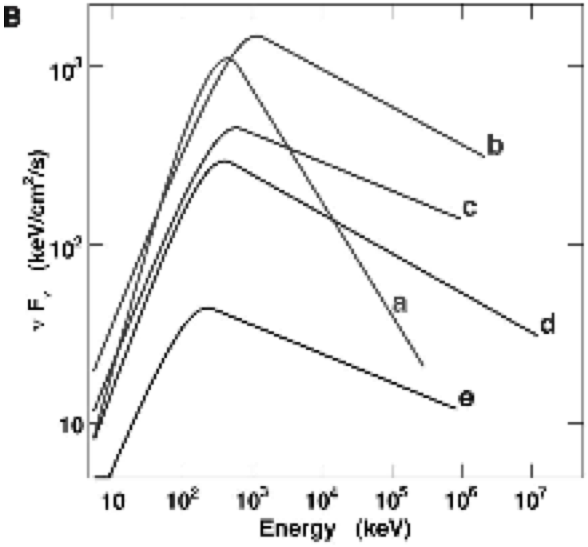

Fermi Surprise: Photosphere component missing

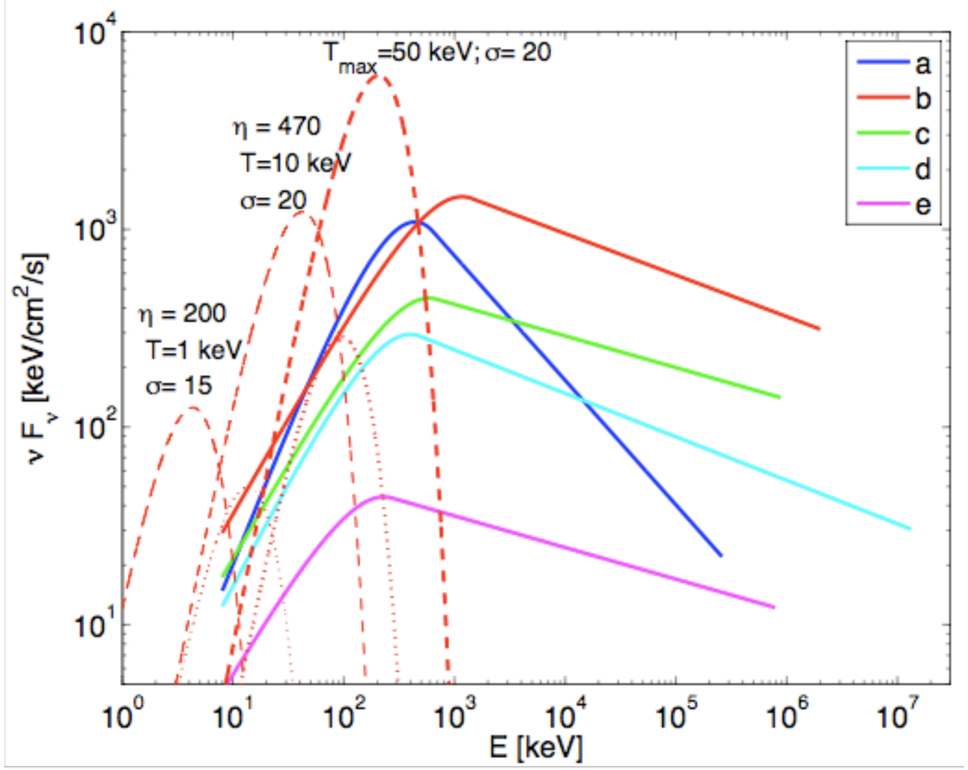

Zhang & Pe'er (2009)

Sigma: ratio between Poynting flux and baryonic flux:

Cf. Guiriec et al. (2015)

$\sigma = L_P/L_b$: at least ~ 20, 15 for GRB 080916C

Modified Fireball Model (1)

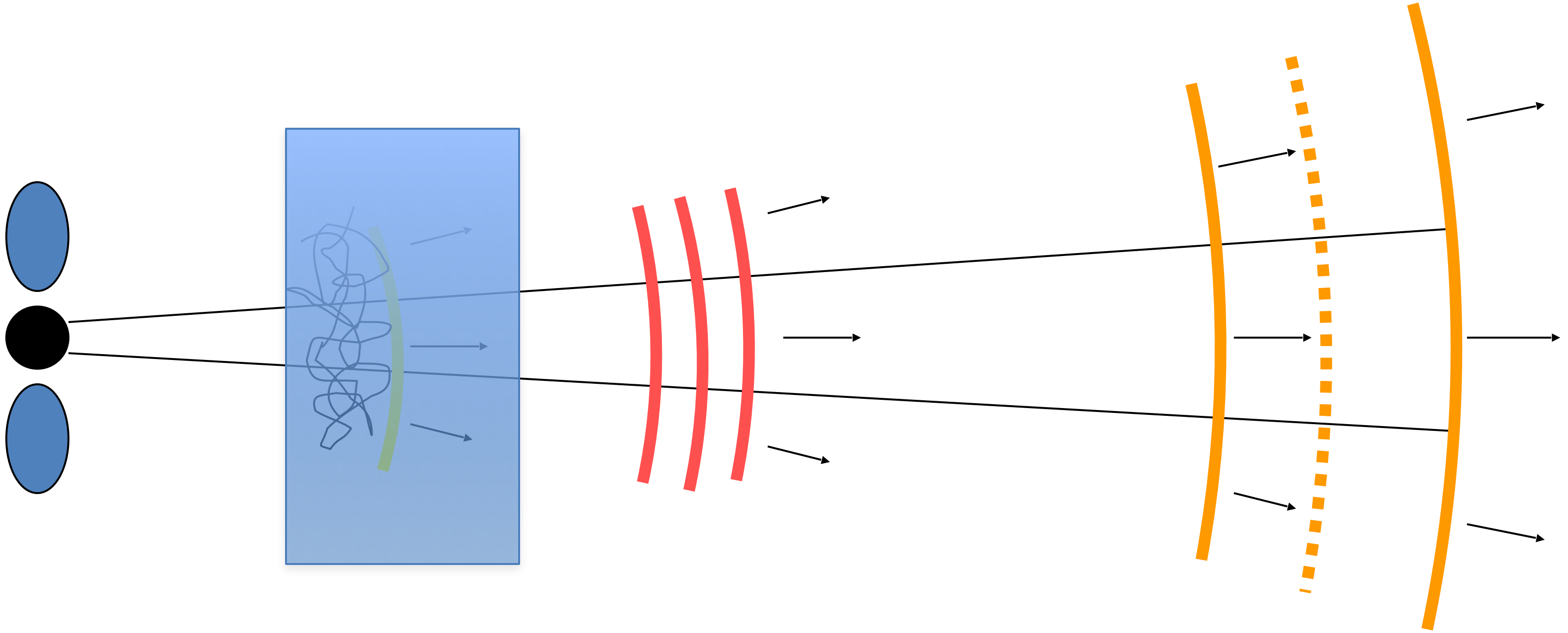

central engine

photosphere

internal shocks

external shocks
(reverse) *(forward)*

GRB prompt emission is from internal shocks
Photosphere emission suppressed

Modified Fireball Model (2)

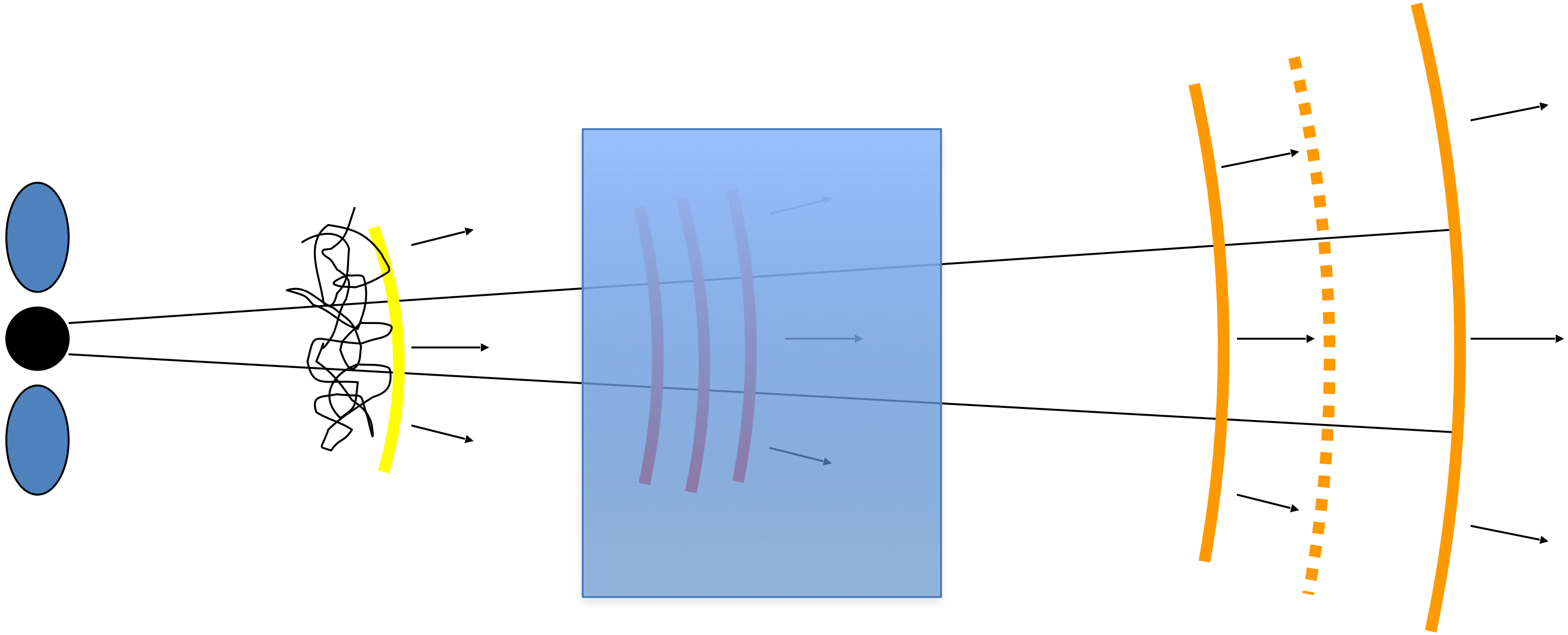

central engine

photosphere

internal shocks

external shocks
(reverse) ***(forward)***

GRB prompt emission: from photosphere
Internal shock emission suppressed

The ICMART Model

(Internal Collision-induced MAgnetic Reconnection & Turbulence)

Zhang & Yan (2011)

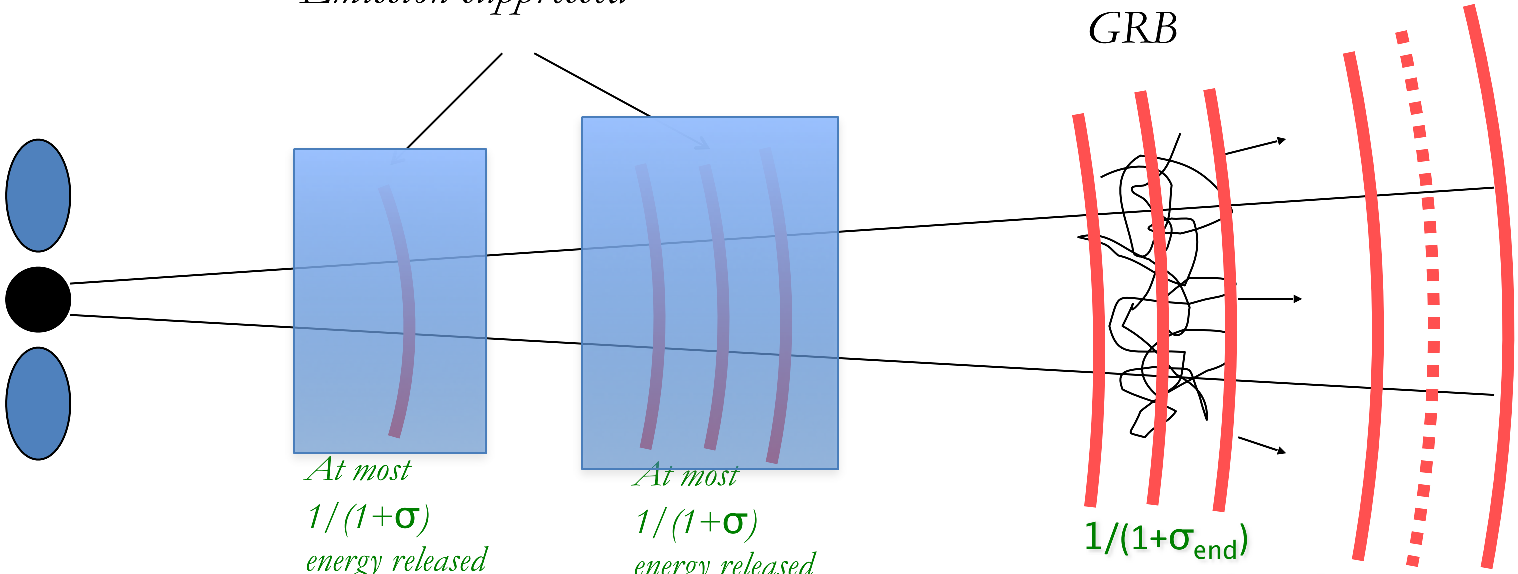

Emission suppressed

GRB

At most
$1/(1+\sigma)$
energy released

At most
$1/(1+\sigma)$
energy released

$1/(1+\sigma_{end})$
energy released

central engine
R ~ 10^7 cm
$\sigma = \sigma_0 >> 1$

photosphere
R ~ 10^{11} - 10^{12} cm
$\sigma \leq \sigma_0$

early collisions
R ~ 10^{13} - 10^{14} cm
σ ~ 1- 100

ICMART region
R ~ 10^{15} - 10^{16} cm
σ_{ini} ~ 1- 100
$\sigma_{end} \leq 1$

External shock
R ~ 10^{17} cm
$\sigma \leq 1$

cf: Lyutikoc & Blandford (2003)…

Energy Flow in GRBs

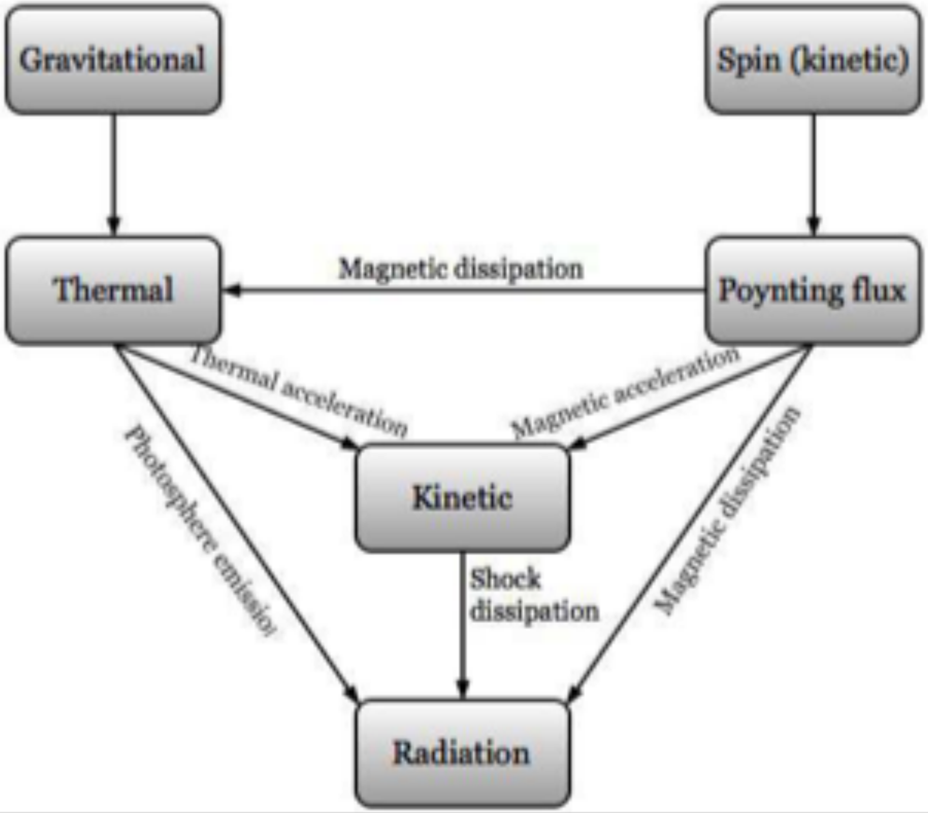

Gravitational

Spin (kinetic)

Thermal

Magnetic dissipation

Poynting flux

Thermal acceleration

Magnetic acceleration

Photosphere emissio

Kinetic

Magnetic dissipation

Shock dissipation

Radiation

Energy Flow in GRBs

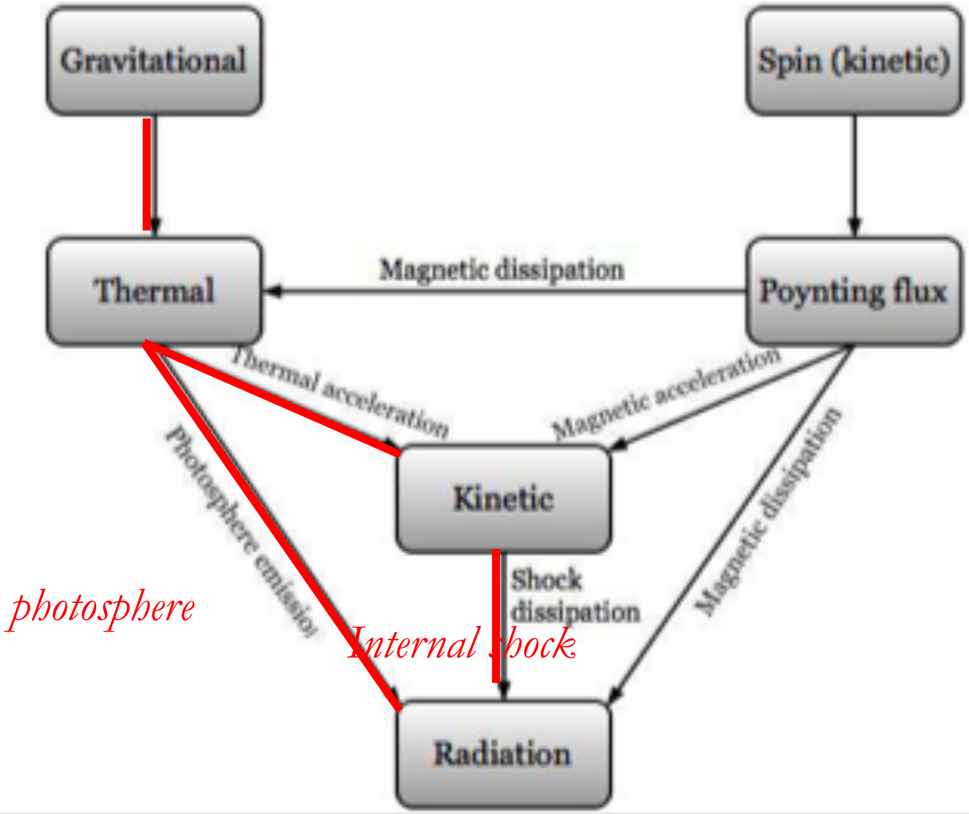

Fireball model

Energy Flow in GRBs

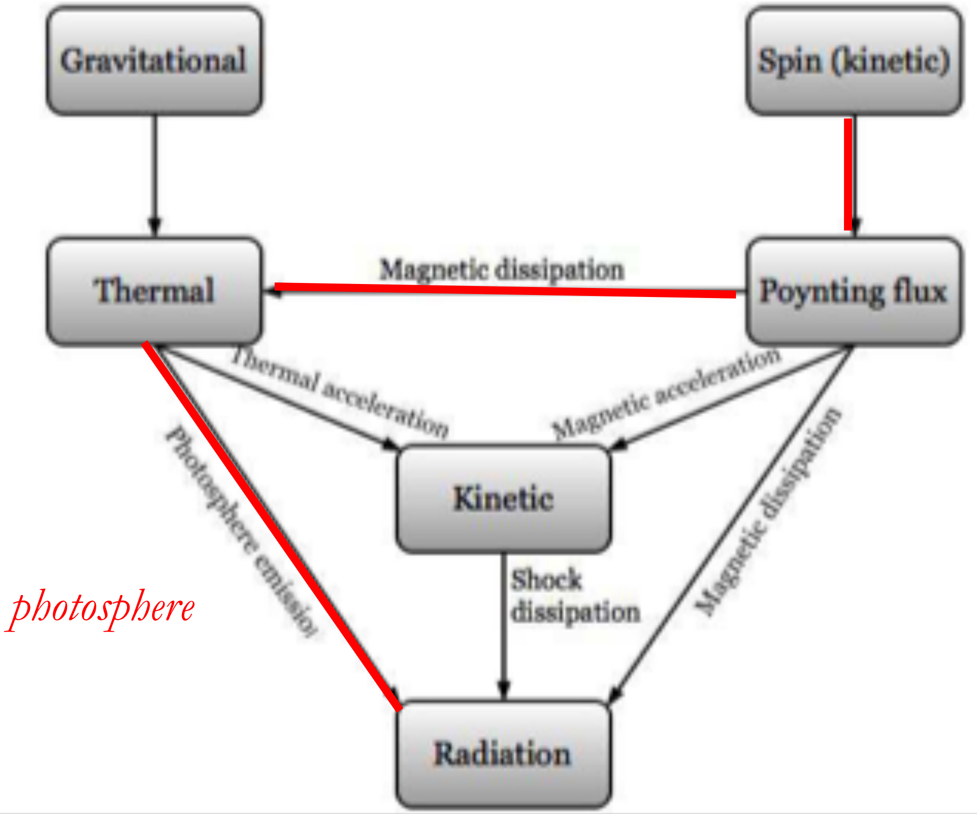

photosphere

Magnetic photosphere model

Energy Flow in GRBs

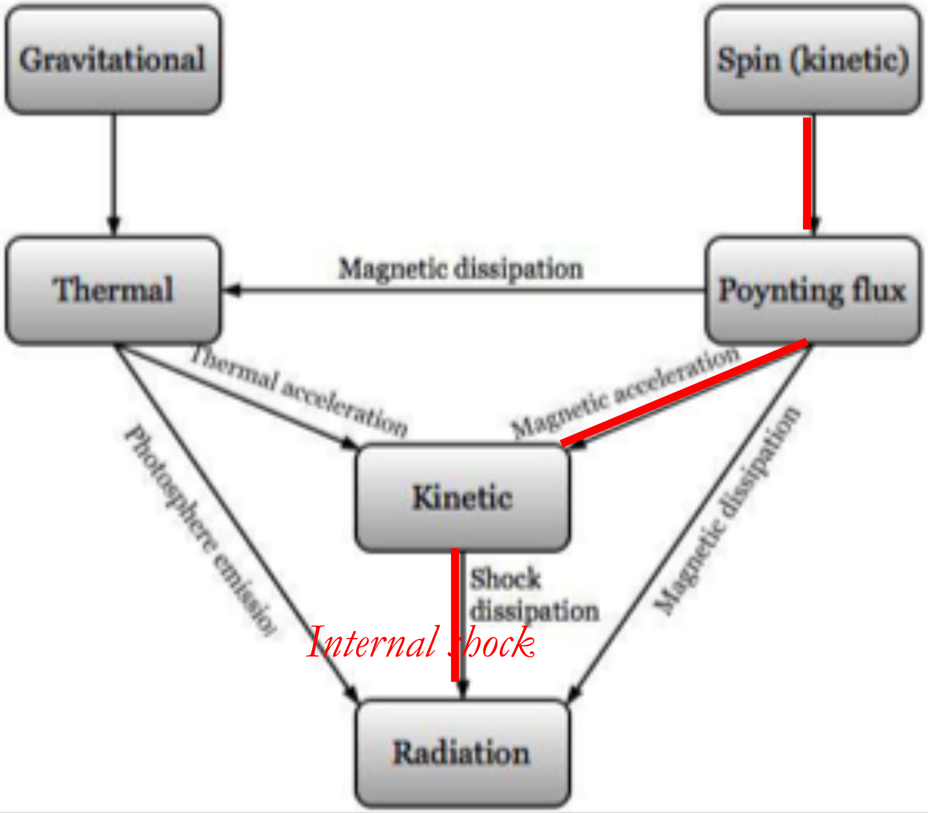

Initially magnetized internal shock model

Energy Flow in GRBs

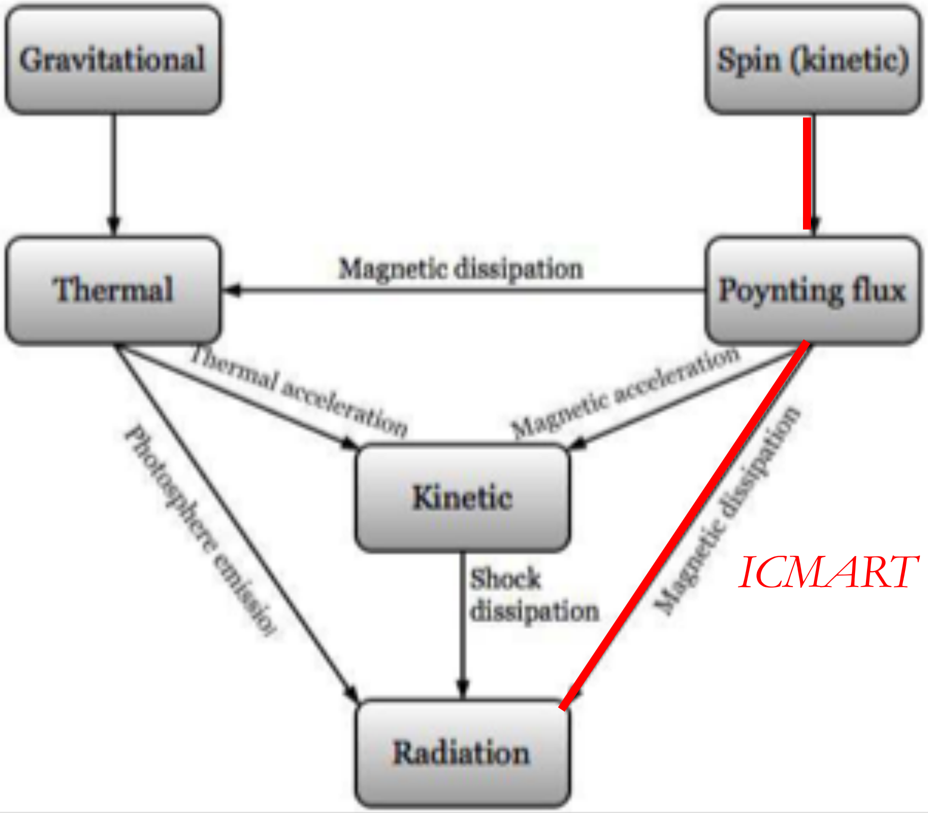

ICMART

Internal collision-induced magnetic reconnection & turbulence (ICMART) model

Energy Flow in GRBs

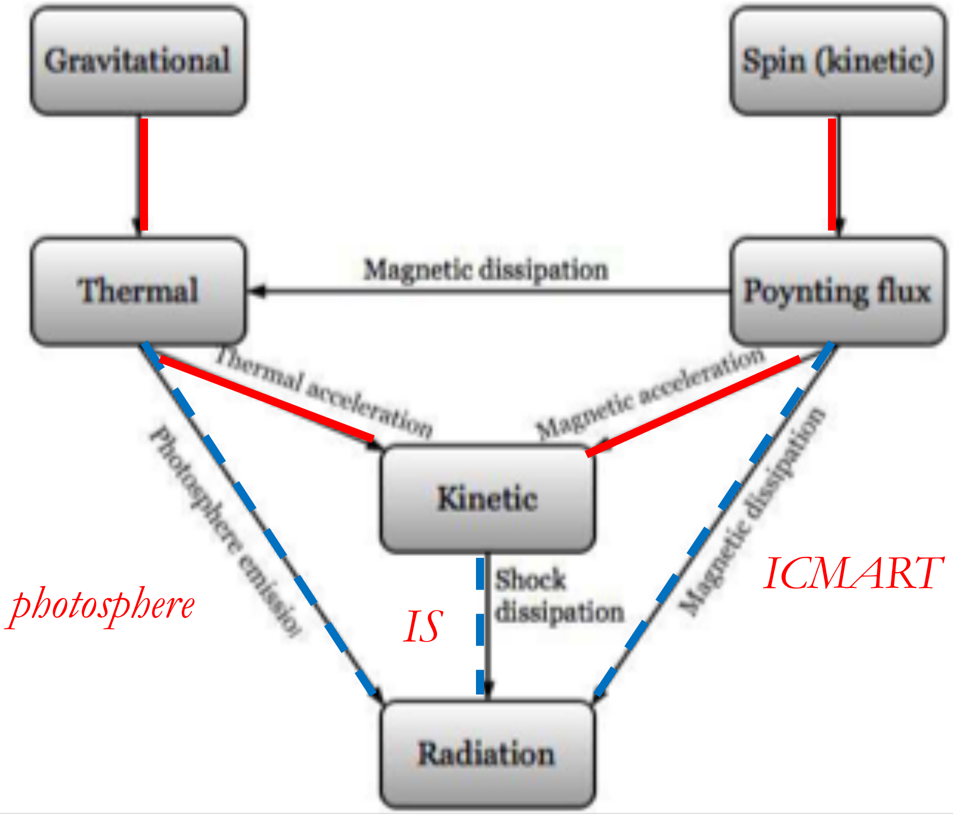

Hybrid models

Fireball: GRB 090902B

(Abdo et al. 2009; Ryde et al. 2010; Zhang et al. 2011; Pe’er et al. 2012)

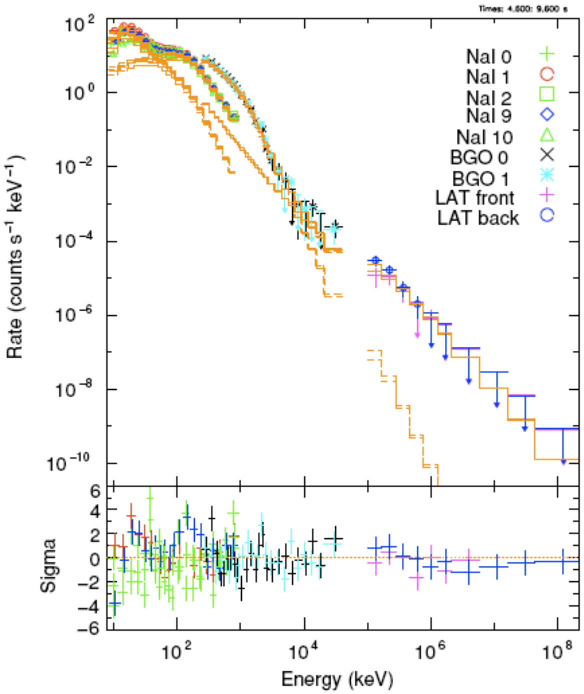

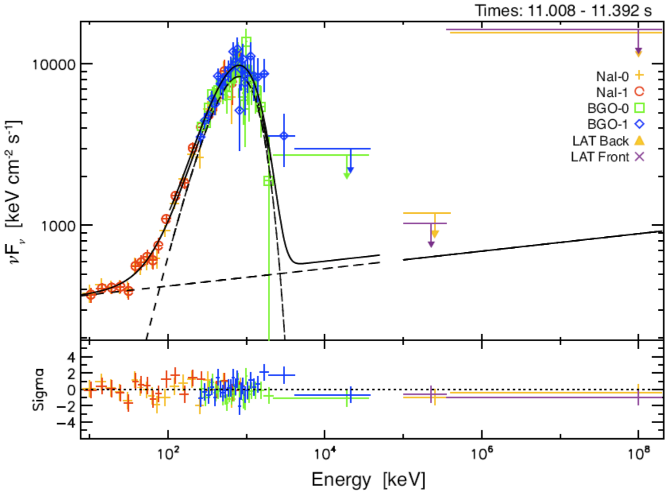

A clear photosphere emission component identified

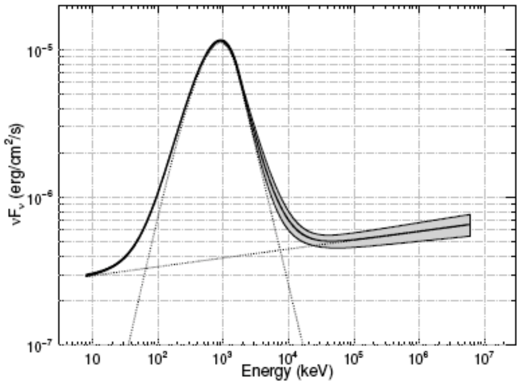

Fireballs do exist!
But are special & rare!

A new high-energy component extending to high energies

Hybrid jets

(Guiriec et al. 2011; Axelsson et al. 2012 …)

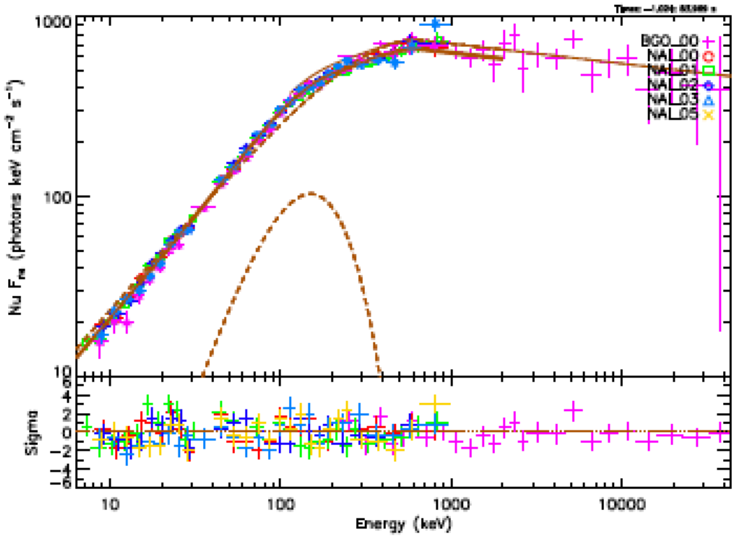

GRB 100724B

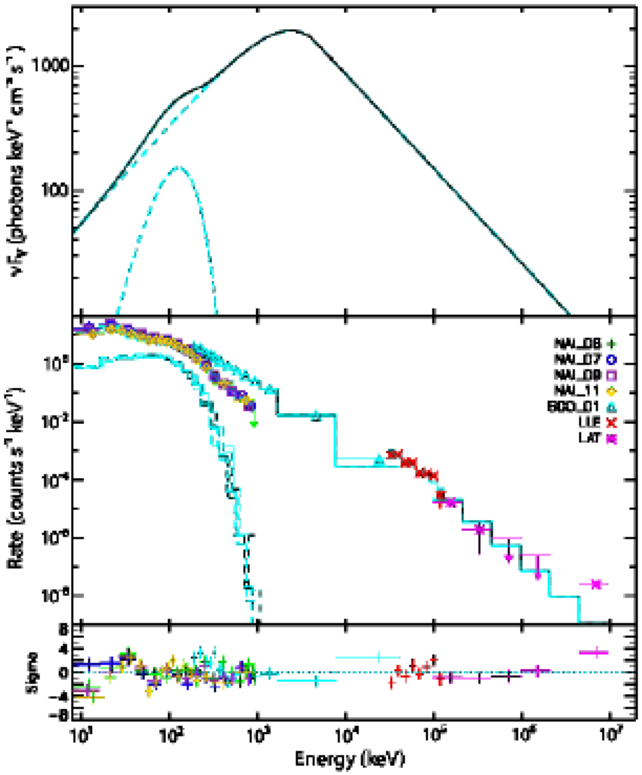

GRB 110721A

Big Picture: GRB jet composition

- GRB jets have diverse compositions:
  - Photosphere dominated (GRB 090902B), rare
  - Intermediate bursts (weak but not fully suppressed photosphere, GRB 100724B, 110721A)
  - Photosphere suppressed, Poynting flux dominated (GRB 080916C)

The majority of GRBs have significant magnetization

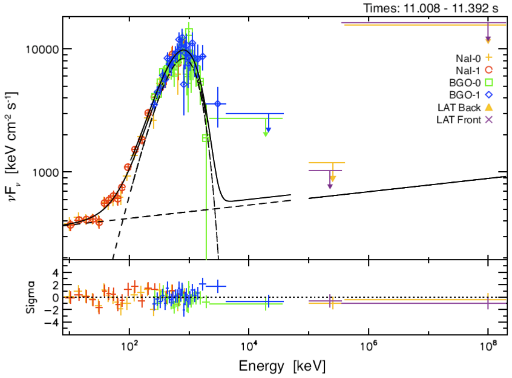

GRB 090902B

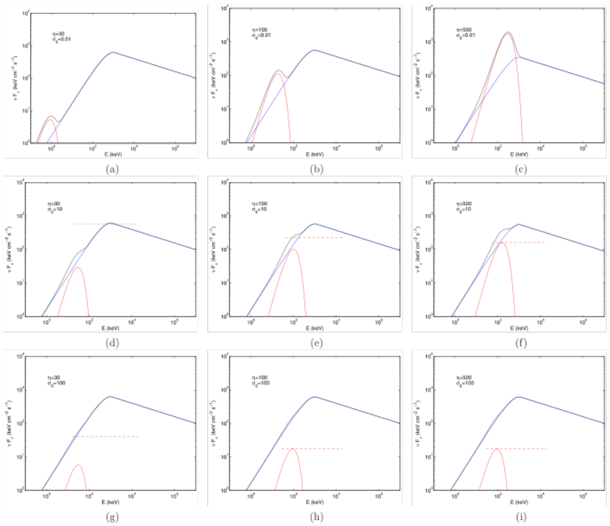

Gao & Zhang 2015

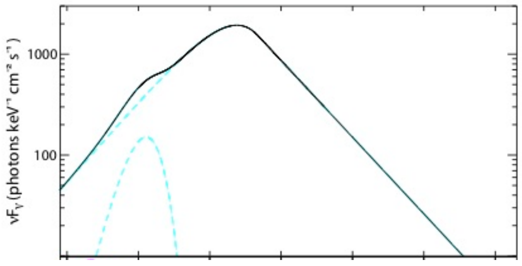

GRB 110721A

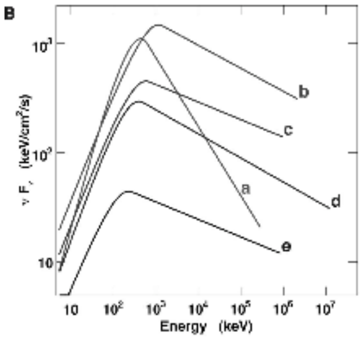

GRB 080916C

Non-detection of neutrinos by IceCube

- Icecube so far has not detected any high-energy neutrino associated with GRBs!
- Consistent with a large emission radius (magnetic dissipation)

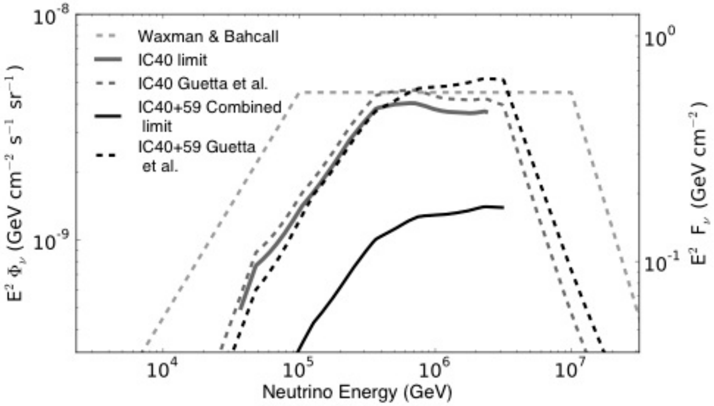

IceCube 2012

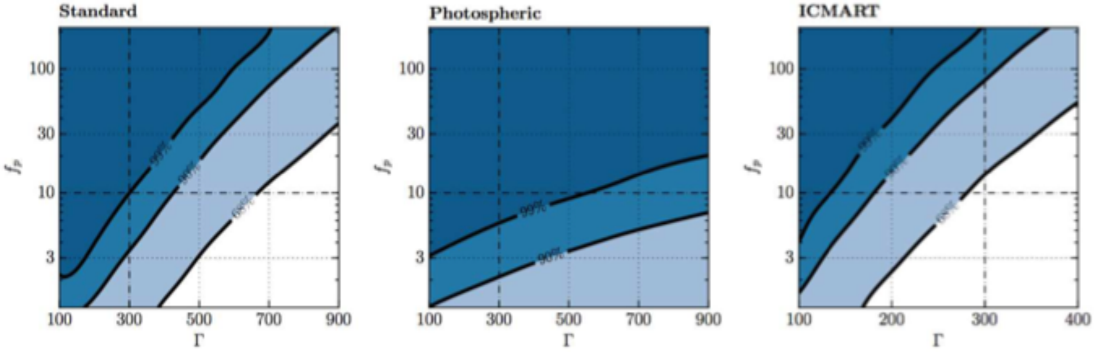

Icecube collaboration 2016

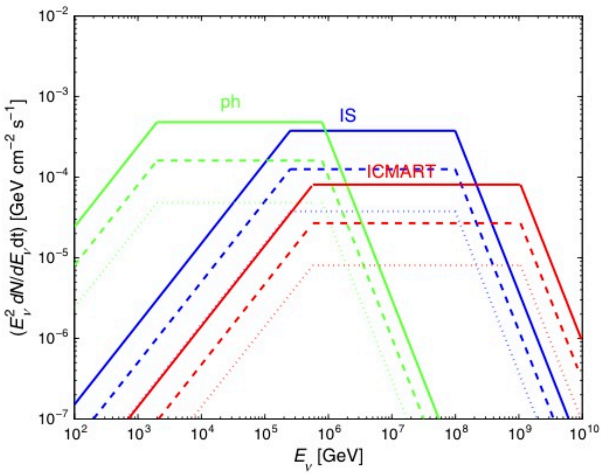

Zhang & Kumar 2013

How?

Radiation Mechanisms (thermal, synchrotron, inverse Compton)

The “Band” function spectrum

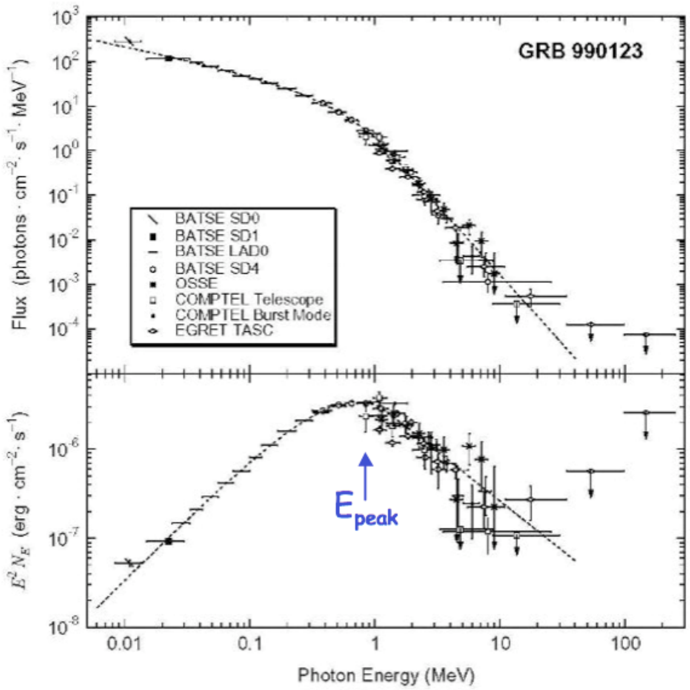

Briggs et al. 1999

David Louis Band (Jan. 9, 1957 – Mar. 16, 2009)

$$N(E) = \begin{cases} A\left(\frac{E}{100\ \mathrm{keV}}\right)^{\alpha} \exp\left(-\frac{E}{E_0}\right), & < (\alpha - \beta)E_0, \\ A\left[\frac{(\alpha-\beta)E_0}{100\ \mathrm{keV}}\right]^{\alpha-\beta} \exp(\beta - \alpha)\left(\frac{E}{100\ \mathrm{keV}}\right)^{\beta}, & \geq (\alpha E- \beta)E_0, \end{cases}$$

Josh Grindley (The 2009 Fermi Symposium, Nov. 2-5, at the David Band special session):
Challenge to theorists: Find the physical meaning of “Band” function in 10 years!

Debate:
What is the origin of the "Band" component?

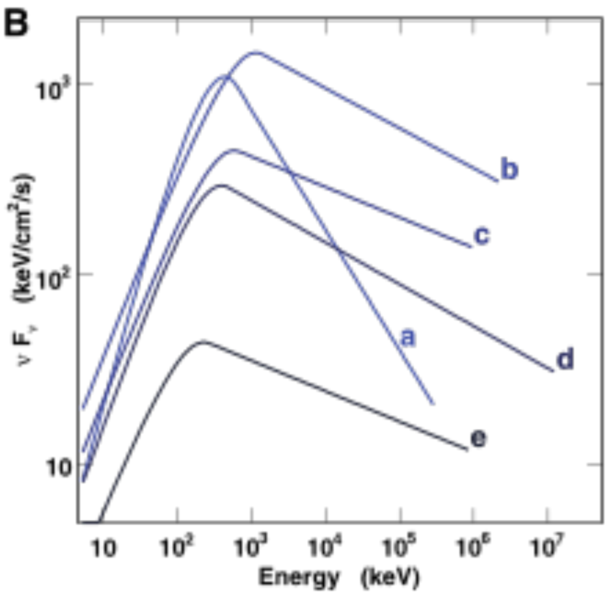

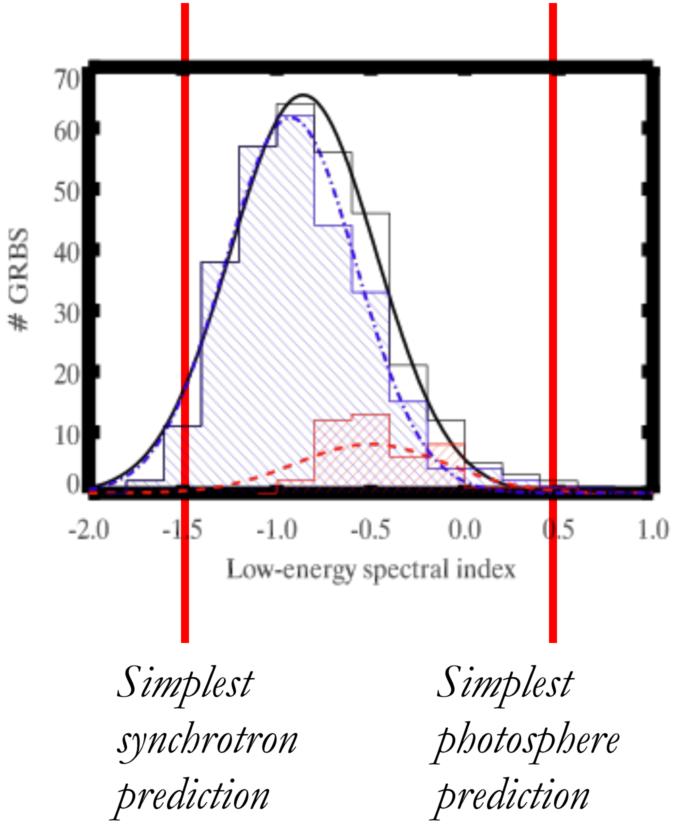

Simplest synchrotron prediction

Simplest photosphere prediction

Nava et al. (2011)

Two distinct views:

- The Band component is the synchrotron emission in optically-thin region.
- The Band component is reprocessed quasi-thermal emission in a dissipative photosphere.

Synchrotron Model: Fast Cooling Spectrum Can Be Harder!

(Uhm & Zhang, 2014, Nature Physics, 10, 351)

- B is decreasing with radius
- Electrons are not in steady state
- Electron spectrum deviates significantly from -2 below the injection energy

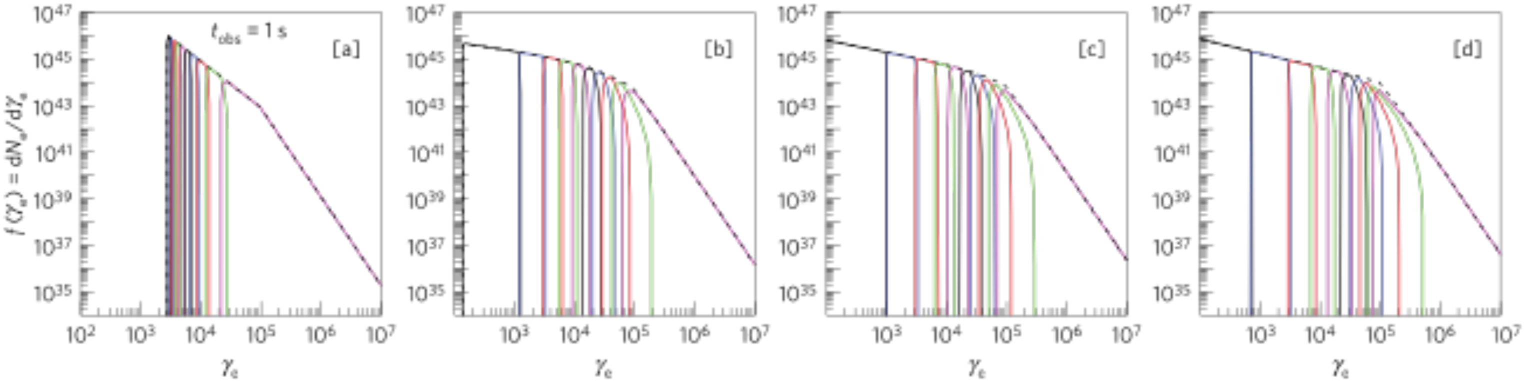

Synchrotron Model: close to (but wider than) the“Band” Function

(Uhm & Zhang, 2014, Nature Physics, 10, 351)

- In the BATSE or GBM band, the spectrum mimics a “Band” function with “correct” indices: α ~ -1, β ~ -2.2

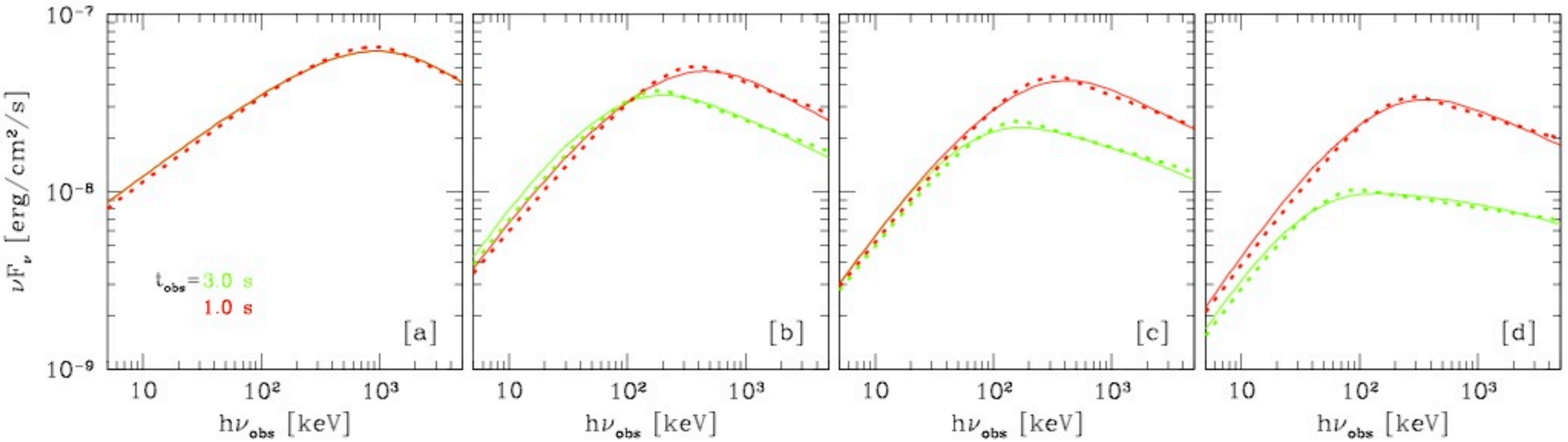

Requirement: Large emission radius where B is low!

“Band” Function is made from synchrotron

(B.-B. Zhang et al., 2016)

- One should apply models directly to data!
- Example: GRB 130606B – no difference between synchrotron and Band models in terms of goodness of fitting

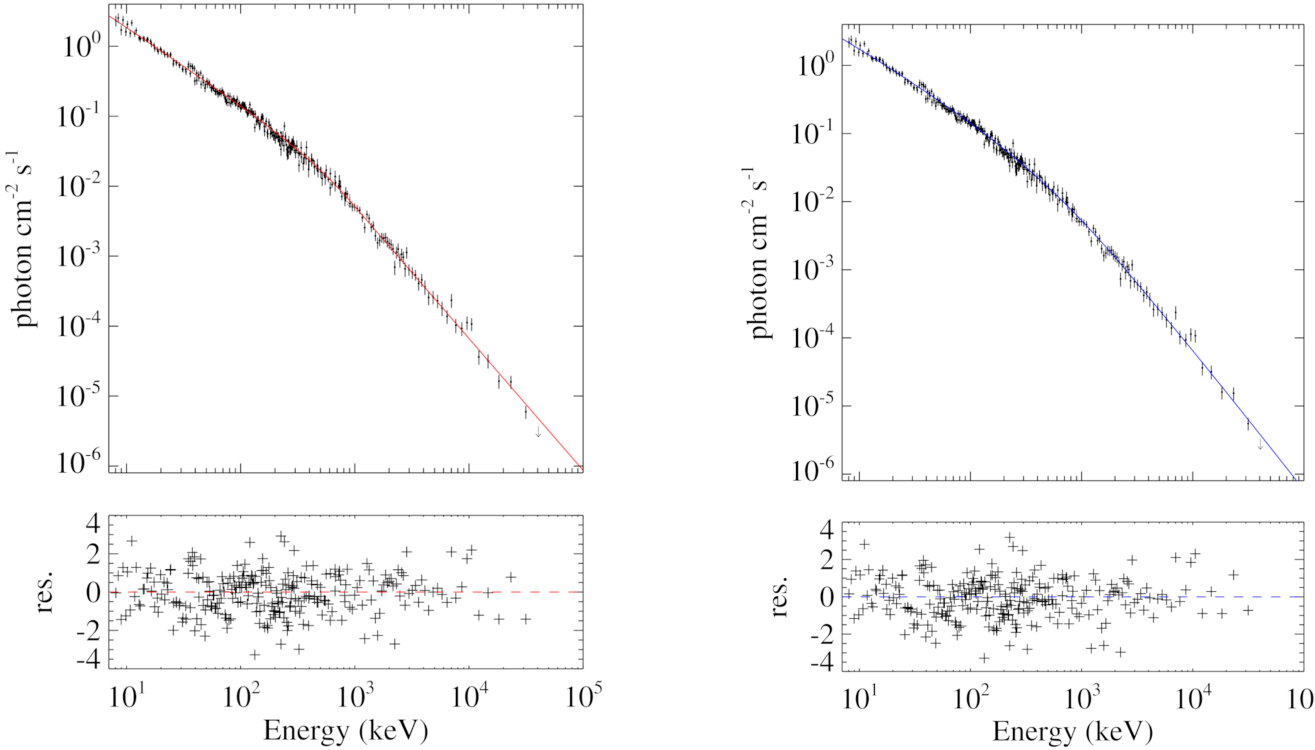

Band & synchrotron model fits

Gamma-ray bursts as cool synchrotron sources

arXiv:1810.06965

J. Michael Burgess[1,2], Damien Bégué[1], Ana Bacelj[1,3], Dimitrios Giannios[4] , Francesco Berlato[1,5], and Jochen Greiner[1,2]

Here we show that idealized synchrotron emission, when properly incorporating time-dependent cooling of the electrons, is capable of fitting ~95% of all time-resolved spectra of single-peaked GRBs as measured with Fermi/GBM. The comparison with spectral fit results based on previous empirical models demonstrates that the past exclusion of synchrotron radiation as an emission mechanism derived via the line-of-death was misleading. Our analysis probes the physics of these ultra-relativistic outflows and the

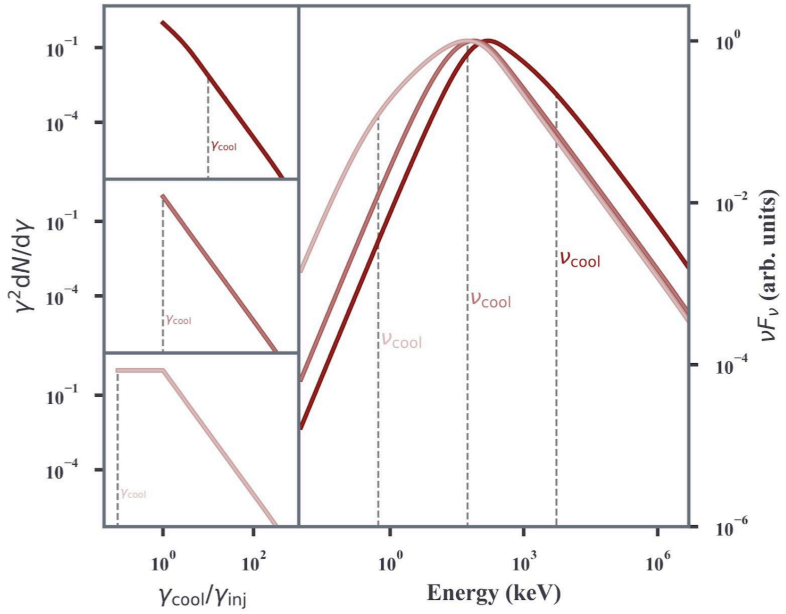

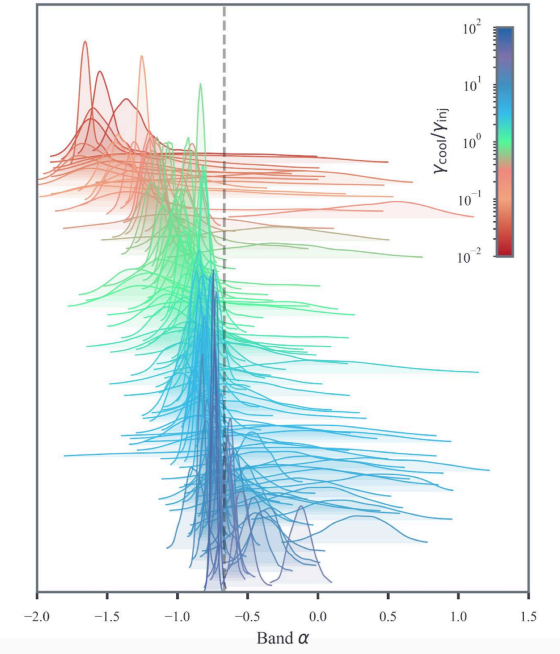

Band Function from Photosphere Emission

- Low-energy photon index
  - Typically hard
  - $F_\nu \sim \nu^{1.5}$ $(\alpha \sim +0.5)$
- May reach -1 in certain structured jets
- Mechanism for 090902B-like GRBs
- To interpret "typical" Band??

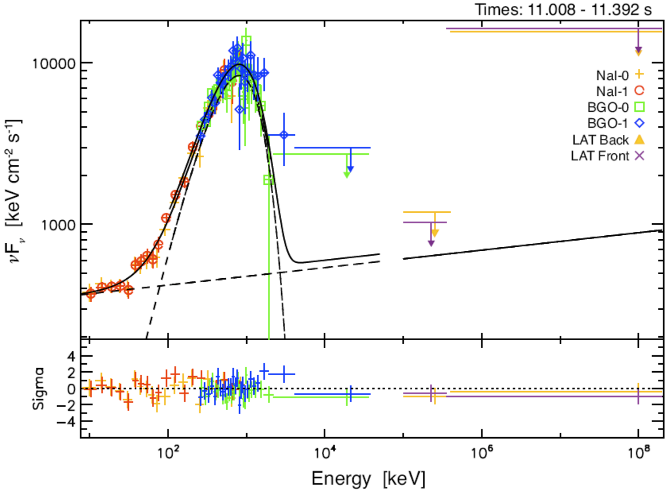

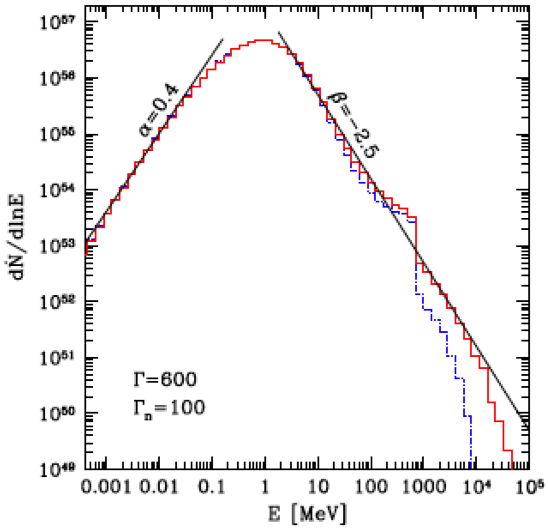

Beloborodov, 2010, MNRAS, 407, 1033

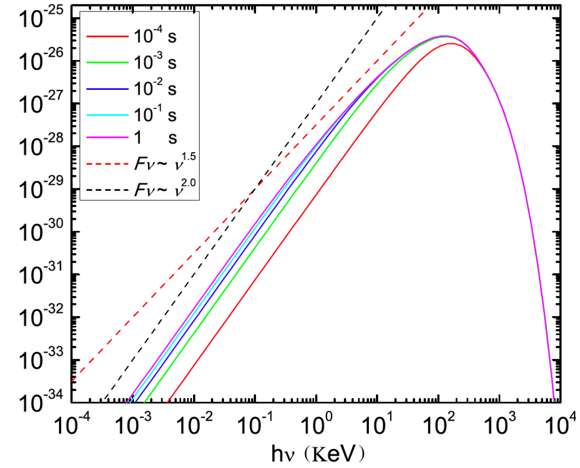

Deng & Zhang, 2014, ApJ, 785, 112

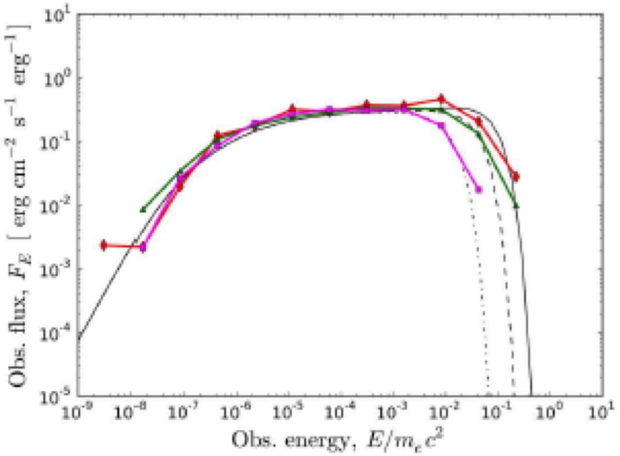

Lundman, Pe'er & Ryde, 2013, MNRAS, 428, 2430

Where?

Emission site (photosphere, internal shocks, larger radii)

Prompt GRB Emission: a Mystery

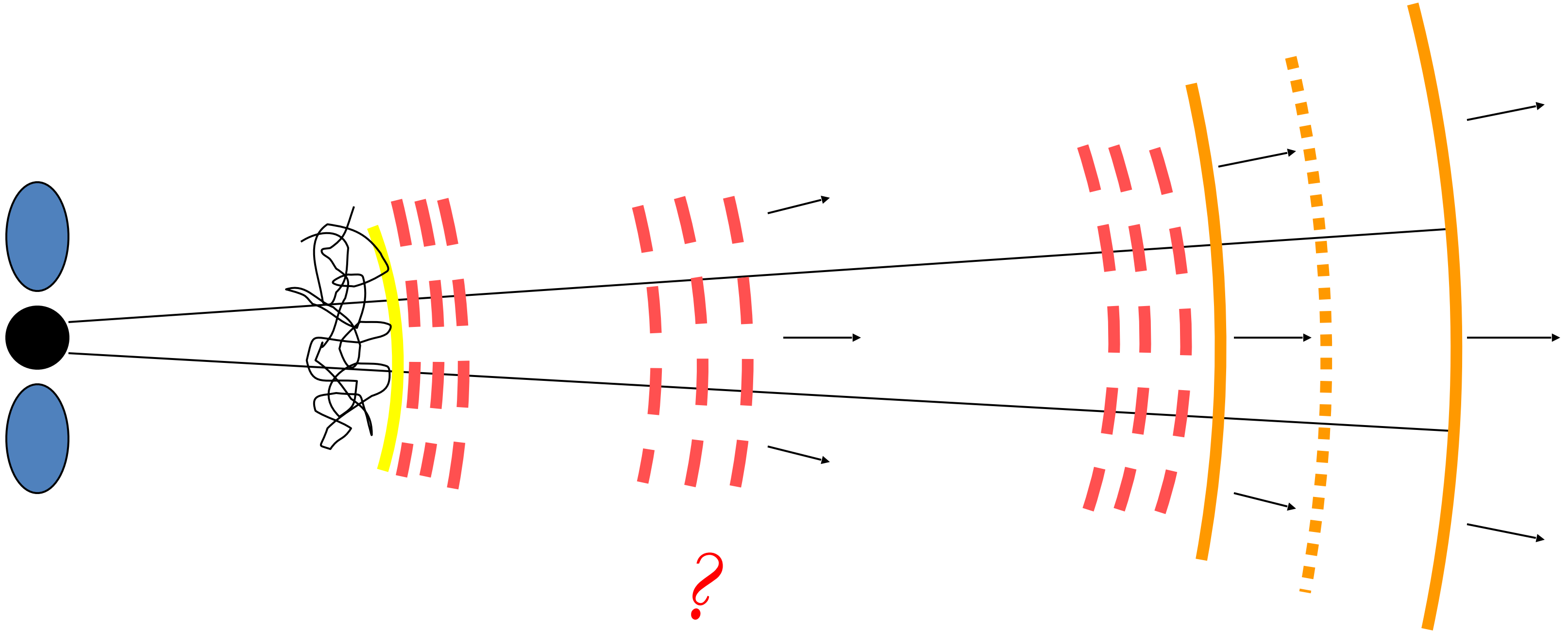

central engine ***photosphere*** ***internal*** ***external shocks***

(reverse) ***(forward)***

What is the jet composition (baryonic vs. Poynting flux)?
Where is (are) the dissipation radius (radii)?
How is the radiation generated (synchrotron, Compton scattering, thermal)?

Smoking gun #1:
GRB pulses, Spectral lags & Ep evolutions

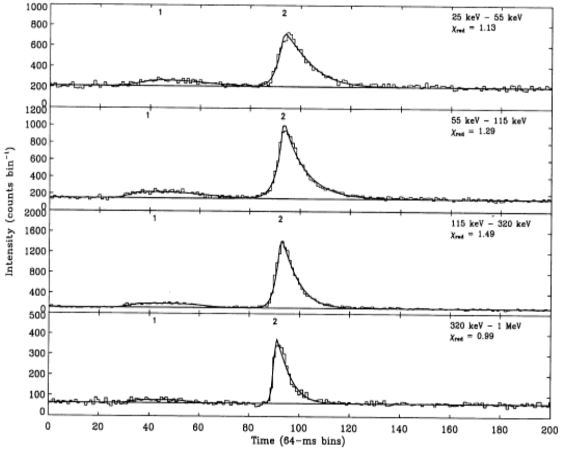

FIG. 16.—BATSE trigger 999: a simple burst profile, with two fitted pulses. Both pulses, identified in all four channels, are considered separable since their overlap is insignificant.

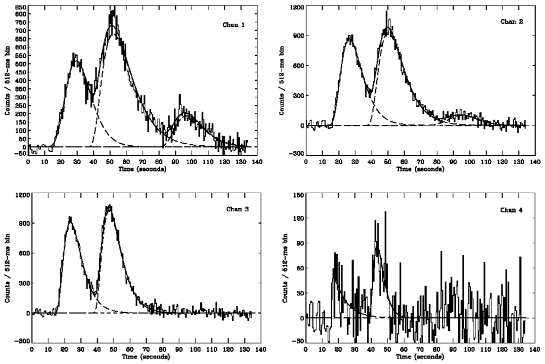

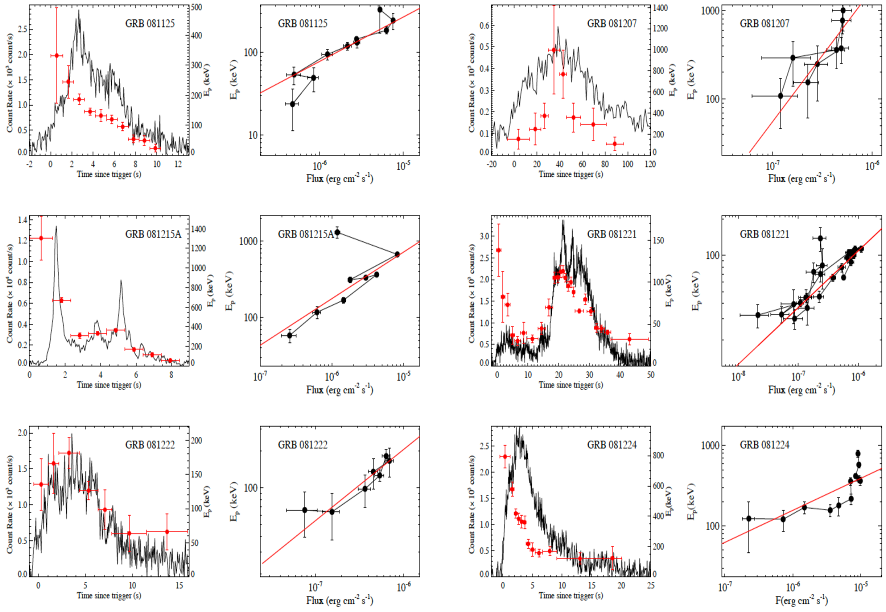

(Lu et al. 2012)

Norris et al. (1996)

Spectral lags & Ep evolutions

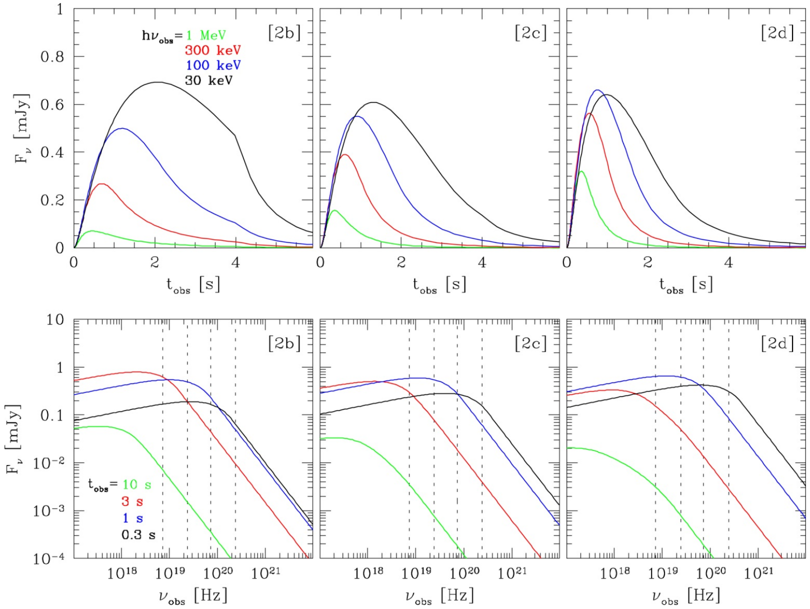

Uhm & Zhang (2016)

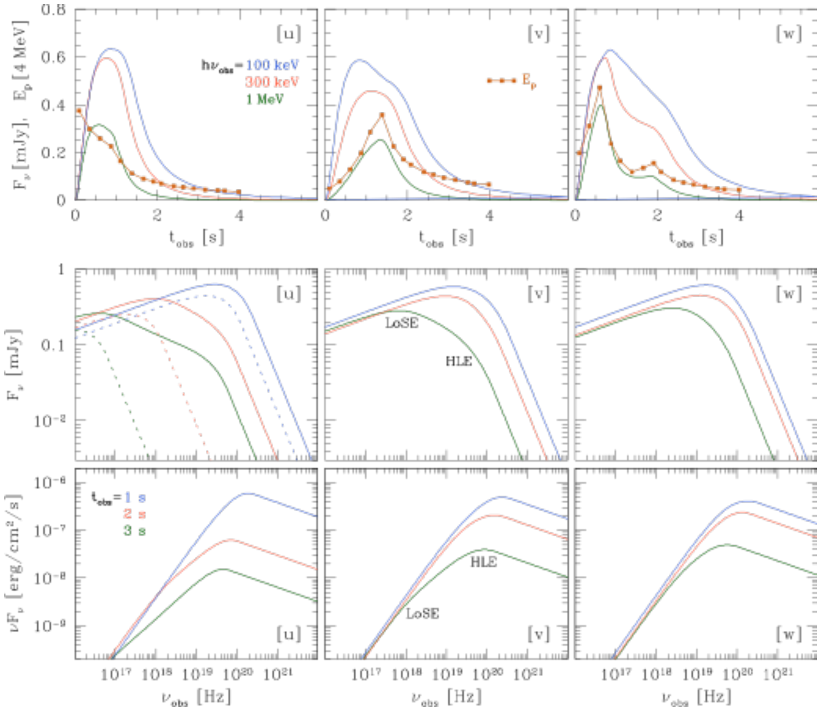

Uhm, Zhang & Racusin (2018)

Model requirements:

1. **Large emission radius**
2. **Bulk acceleration**

$$r \sim \Gamma^2 c\, t_{\rm pulse} \sim (3 \times 10^{14}\ {\rm cm})\,\Gamma_2^2 (t_{\rm pulse}/1\ {\rm s}).$$

Bulk acceleration & “dark energy”

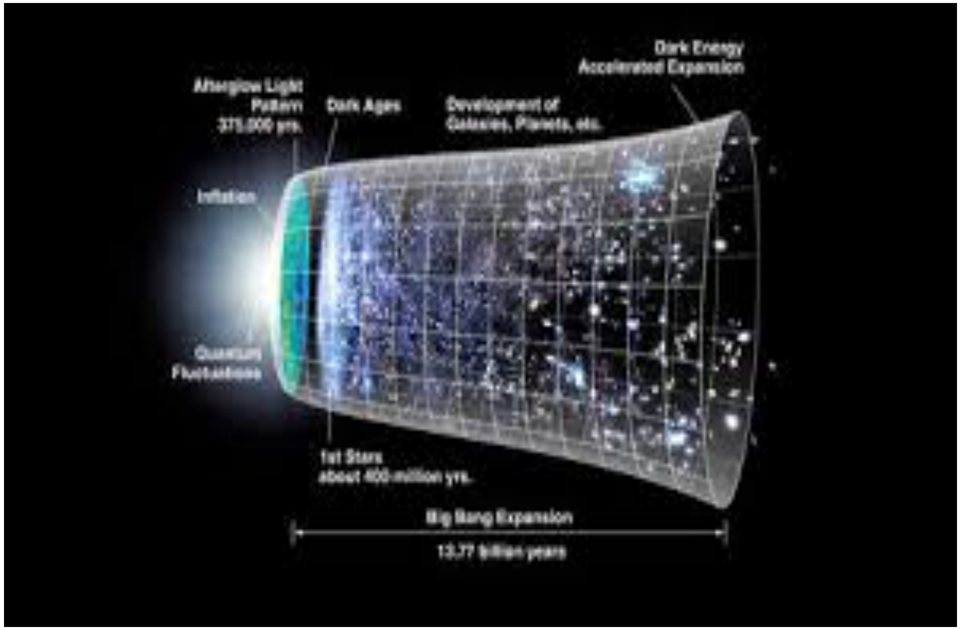

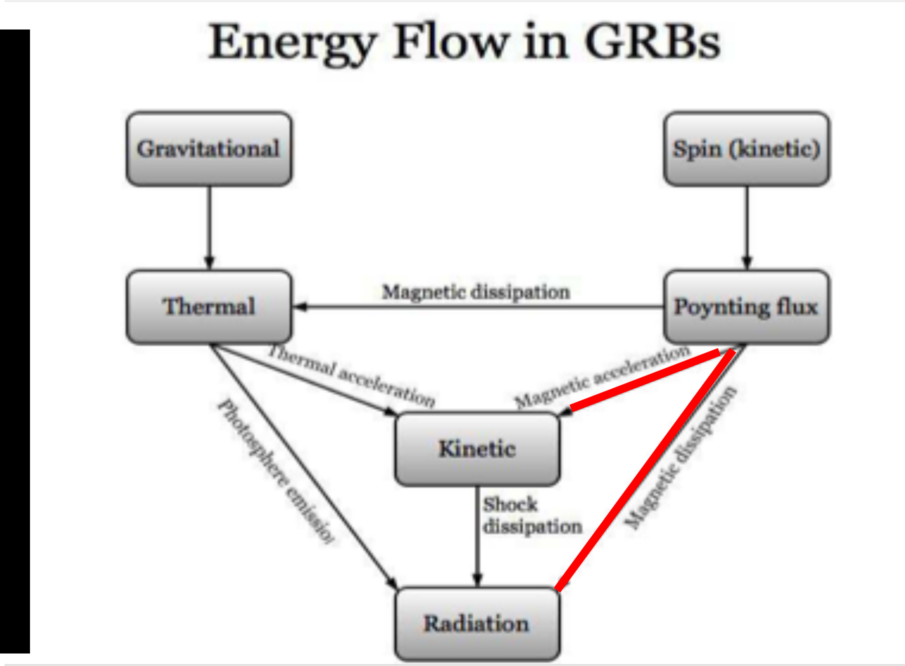

Smoking gun of Poynting flux dissipation:
bulk acceleration in the emission region

Smoking gun #2:
High-latitude emission & curvature effect

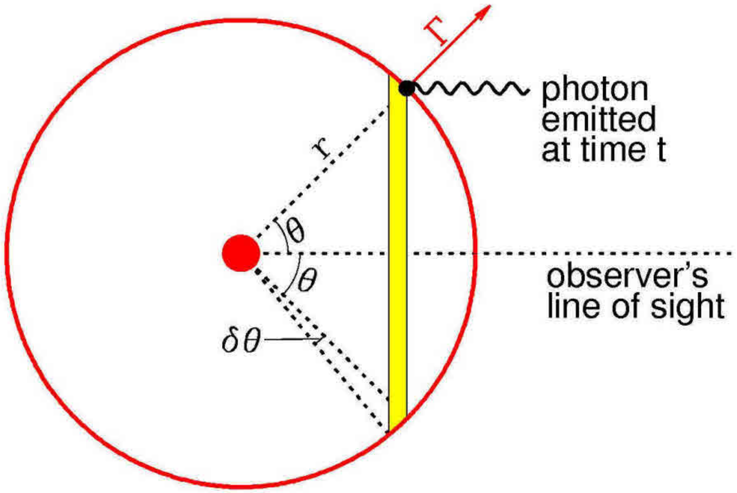

- Predicted features:
  - Lightcurve:

$$F_{\nu_{\rm obs}}^{\rm obs} \propto t_{\rm obs}^{-\hat{\alpha}} \, \nu_{\rm obs}^{-\hat{\beta}},$$

$$\hat{\alpha} = 2 + \hat{\beta},$$

Kumar & Panaitescu (2000)

  - Spectral (more clean test):

$$F_{\nu,E_p} \propto E_p^2$$

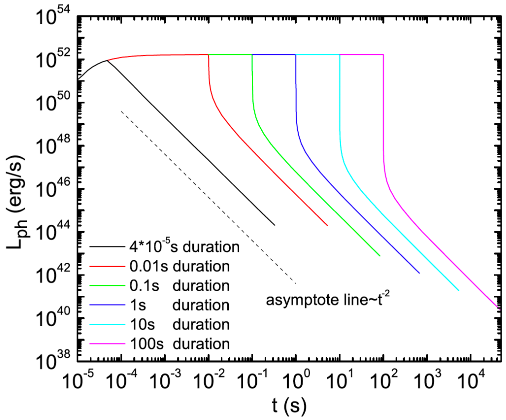

Not detectable for photosphere emission
Deng & Zhang, 2014

High-latitude emission in prompt emission

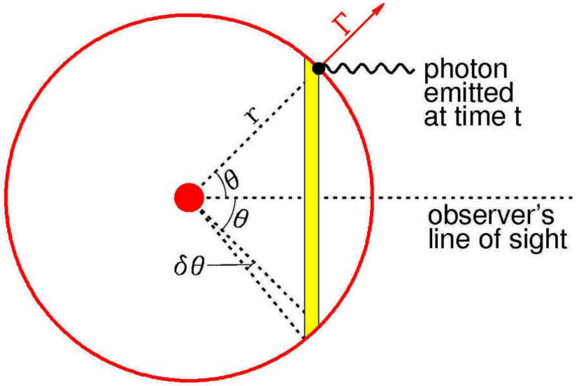

- Direct & clean test:

$$F_{\nu,E_p} \propto E_p^2$$

Directly detected in a good sample of long GRBs

Uhm et al. (2019); Tak et al. (2019)

Model requirements:
Large emission radius

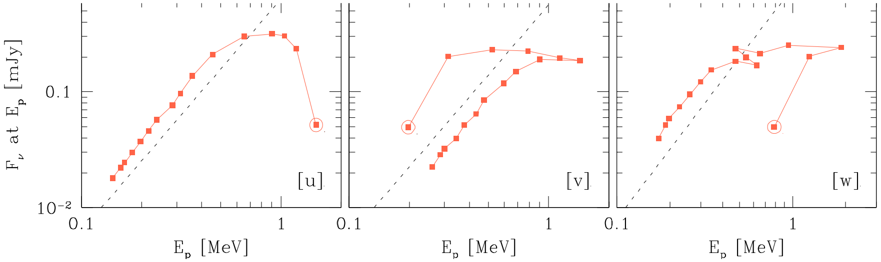

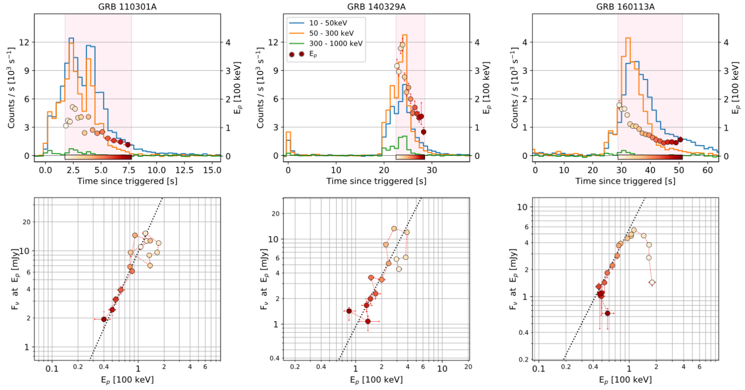

The ICMART Model

(Internal Collision-induced MAgnetic Reconnection & Turbulence)

Zhang & Yan (2011)

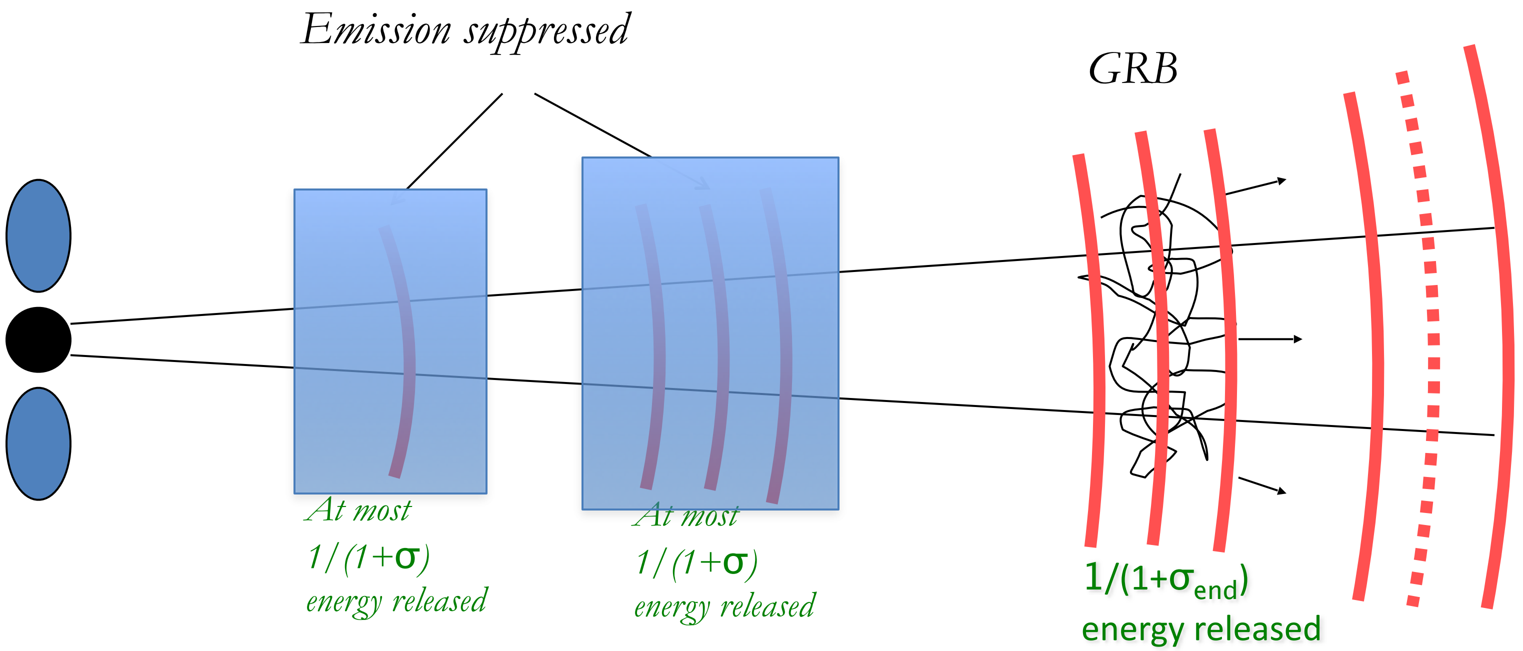

Emission suppressed

GRB

At most
$1/(1+\sigma)$
energy released

At most
$1/(1+\sigma)$
energy released

$1/(1+\sigma_{end})$
energy released

central engine
R ~ 10^7 cm
$\sigma = \sigma_0 >> 1$

photosphere
R ~ 10^{11} - 10^{12} cm
$\sigma \leq \sigma_0$

early collisions
R ~ 10^{13} - 10^{14} cm
σ ~ 1- 100

ICMART region
R ~ 10^{15} - 10^{16} cm
σ_{ini} ~ 1- 100
$\sigma_{end} \leq 1$

External shock
R ~ 10^{17} cm
$\sigma \leq 1$

cf: Lyutikoc & Blandford (2003)…

Progenitors (massive star core collapse vs. neutron star merger)

Two physical types

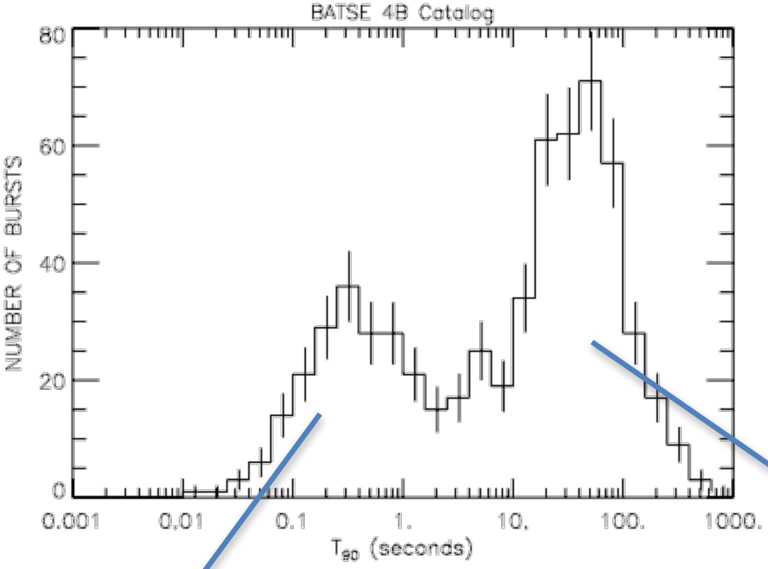

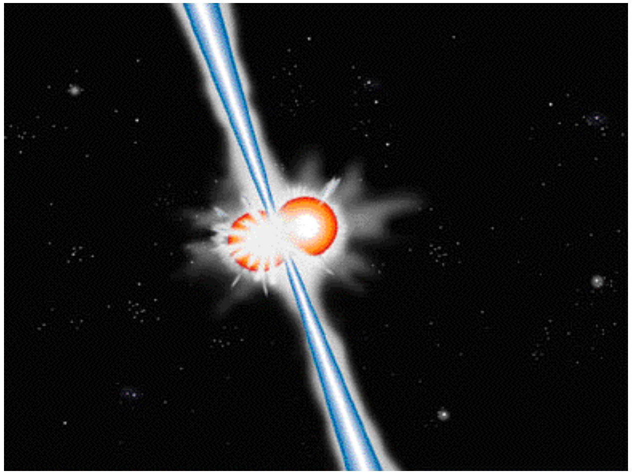

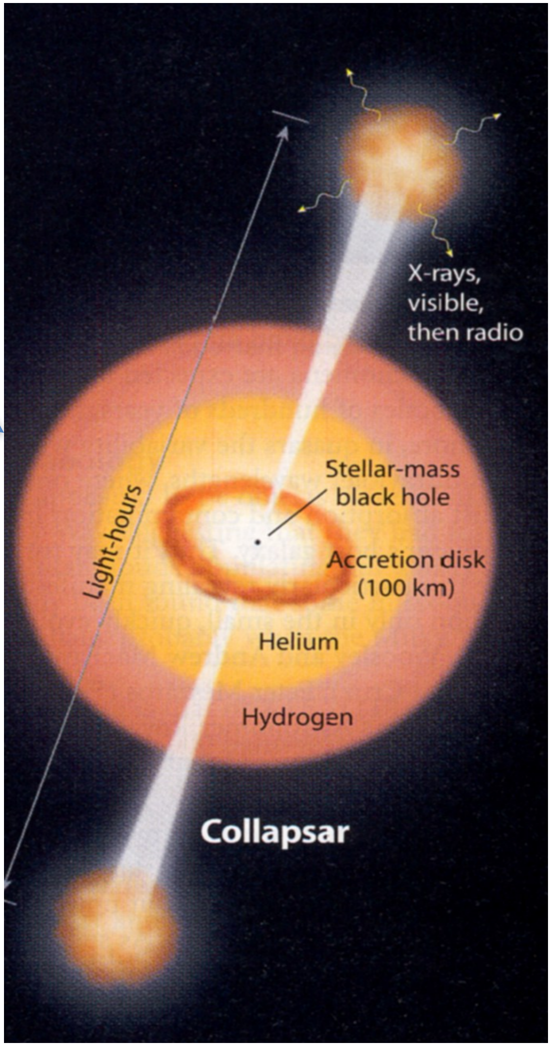

Most beautiful figure in astrophysics: GW170817/GRB 170817A

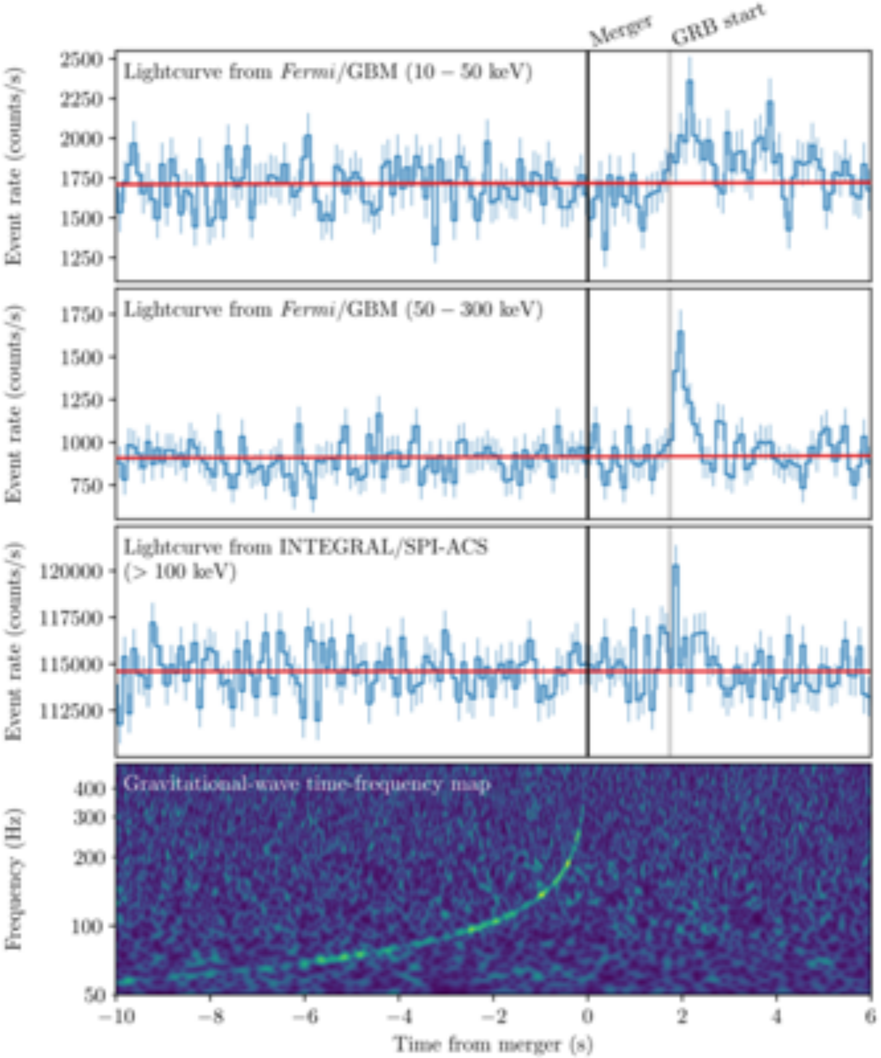

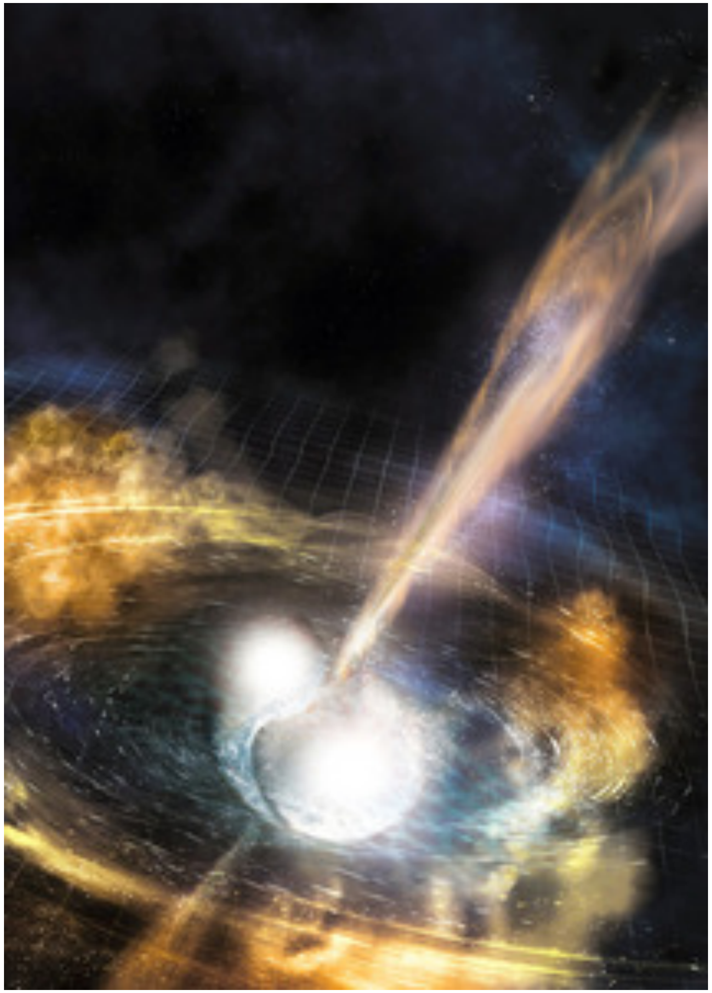

Geometry (uniform vs. structured jet; jet vs. cocoon)

GRB 170817A:

geometric model

Abbott et al. 2017, ApJL, 848, L13; Mooley et al. 2018, Nature, 554, 207; B.-B. Zhang et al. 2018, Nature Communications, 9, 447

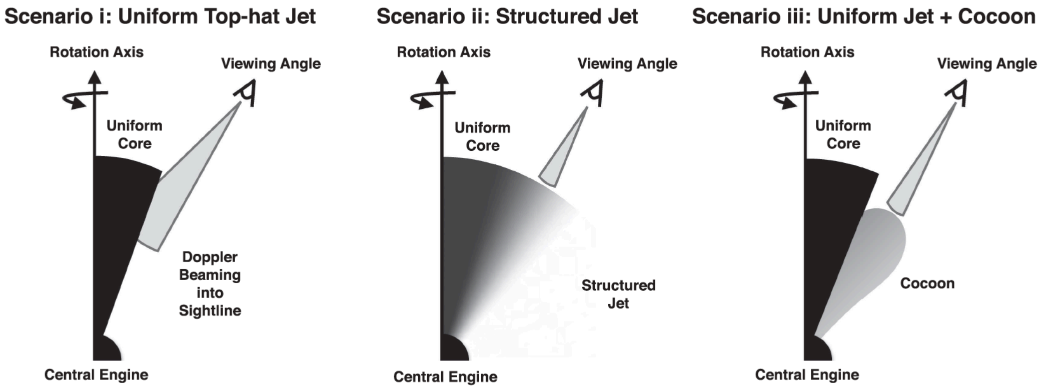

Favored

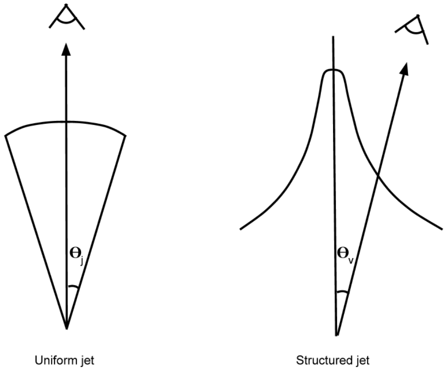

Structured jet: Zhang & Meszaros (2002); Rossi et al. (2002)

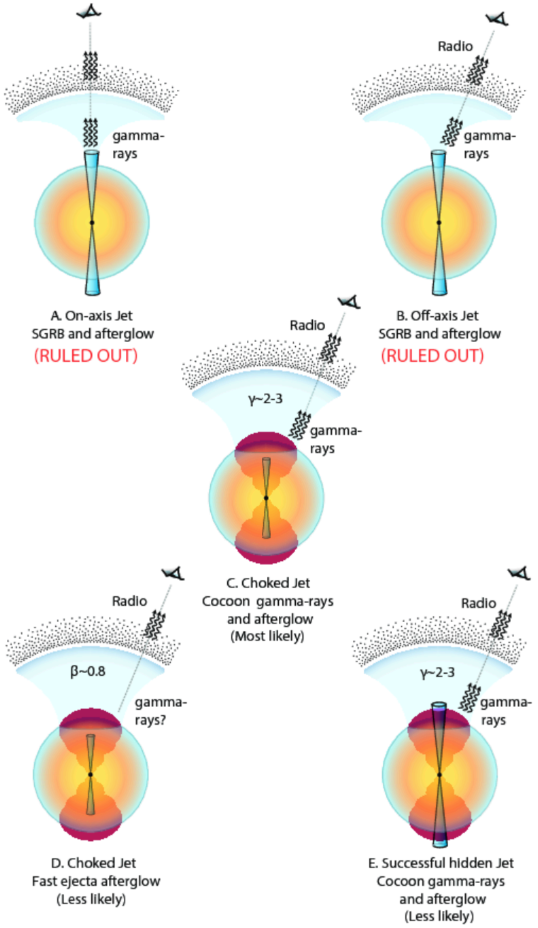

Cocoon shock breakout model, ruled out

Superluminal motion

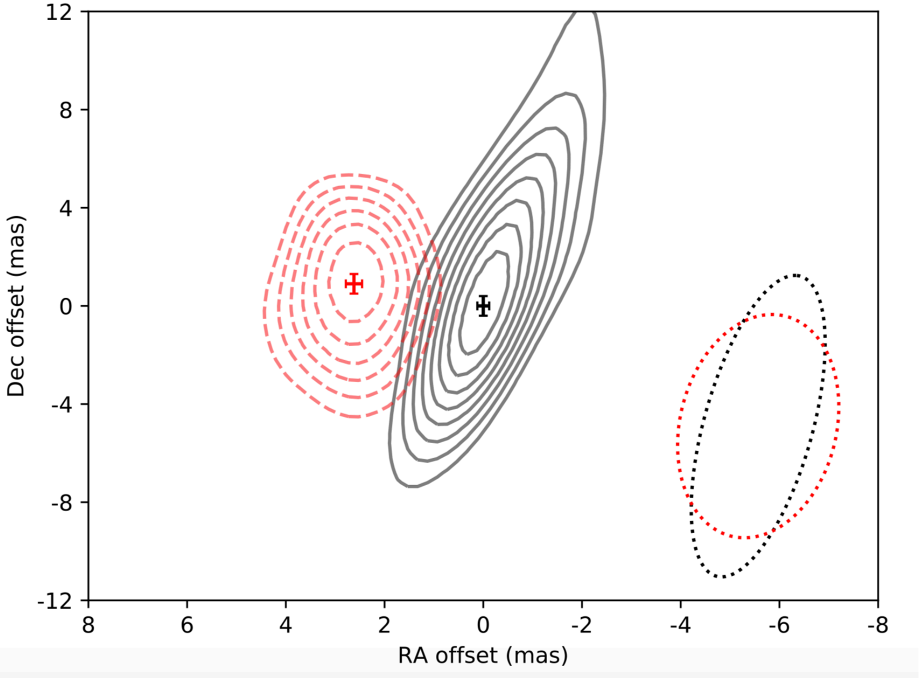

Mooley et al., 2018

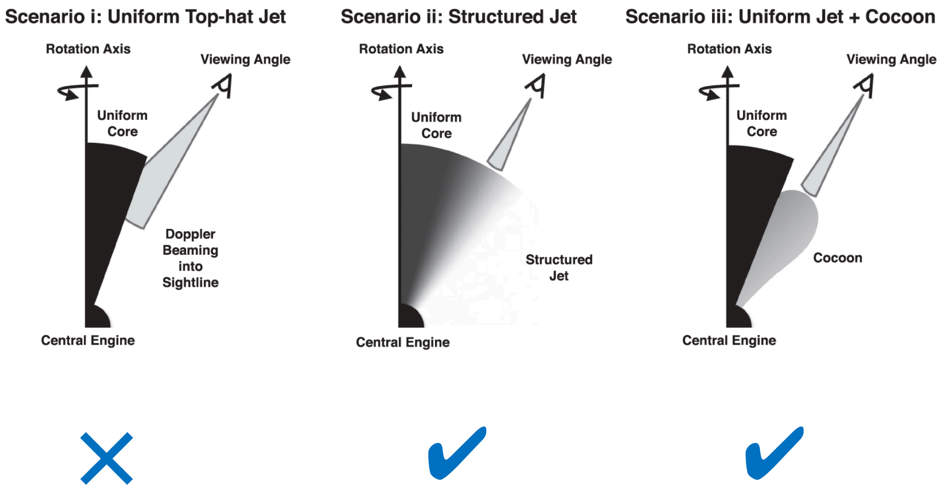

Structured jet or cocoon?

Direct observation of a structured GRB jet for the first time!

Structured jet or cocoon?

Geng et al. 2019, ApJL, 877, L40

See also: Xie et al. 2018, ApJ, 863, 58 *Gottlieb et al. 2018, MNRAS, 479, 588*

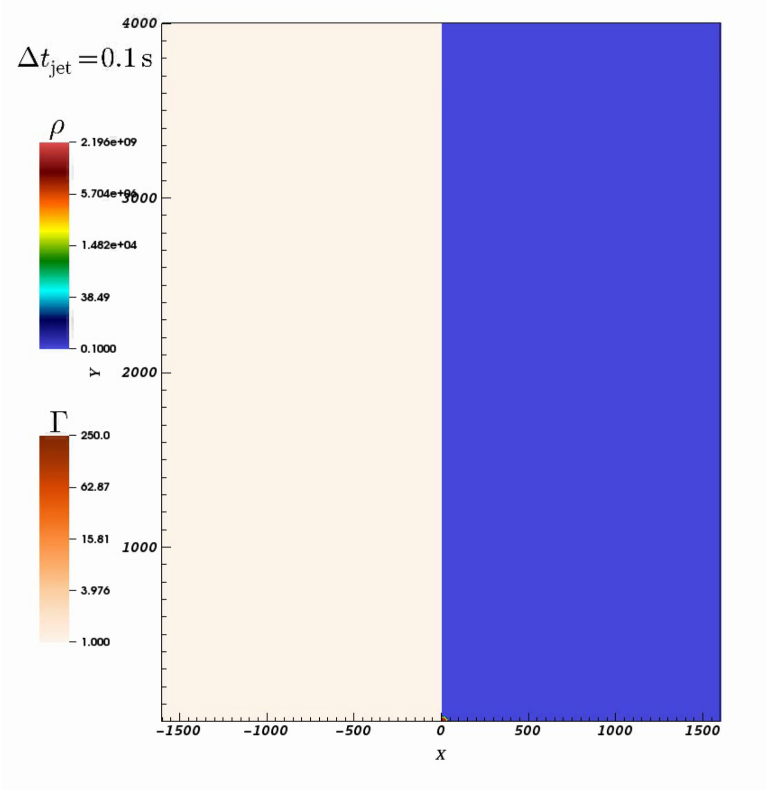

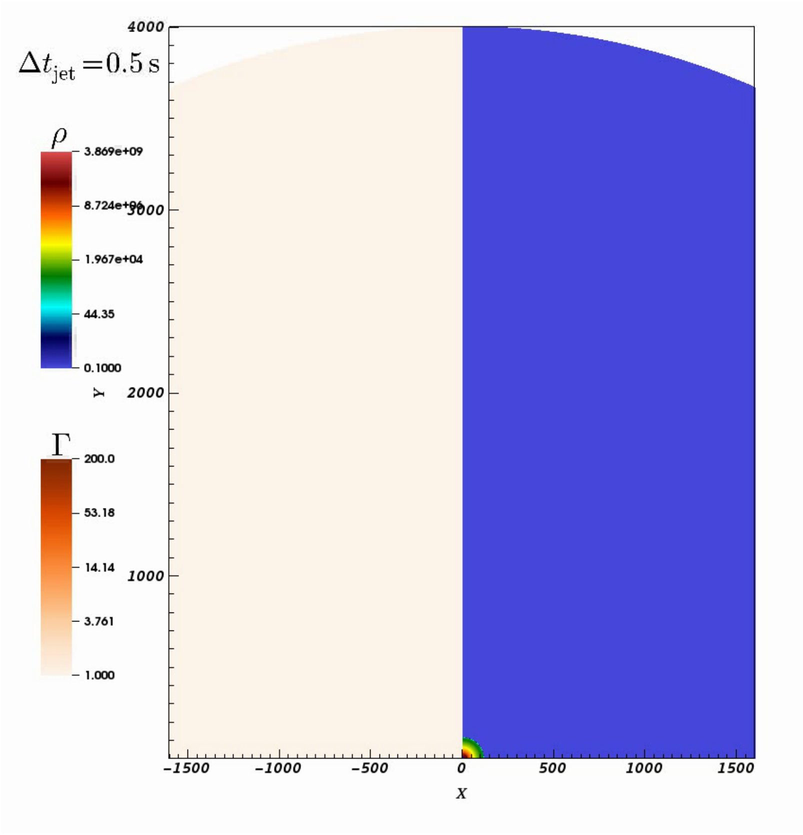

Structured jet or cocoon?

Geng et al. 2019, ApJL, 877, L40

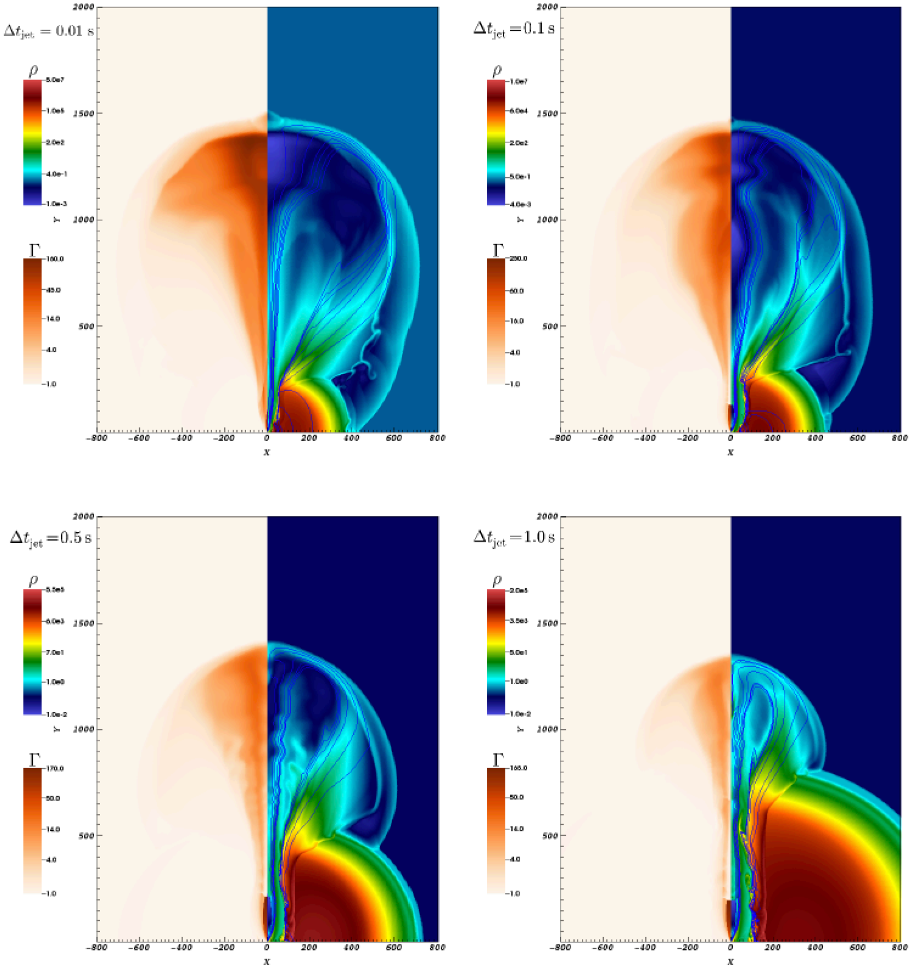

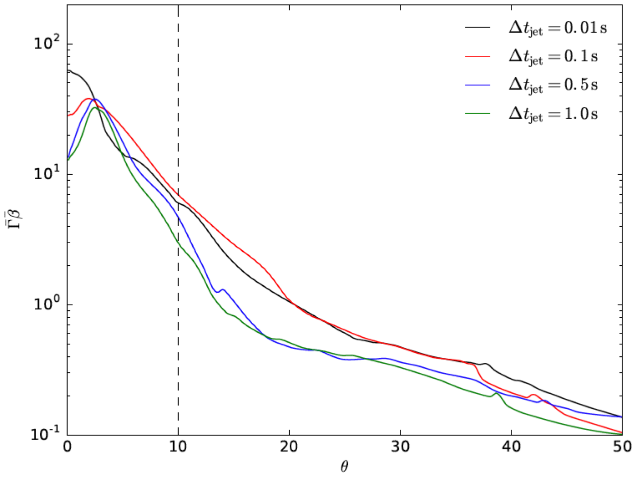

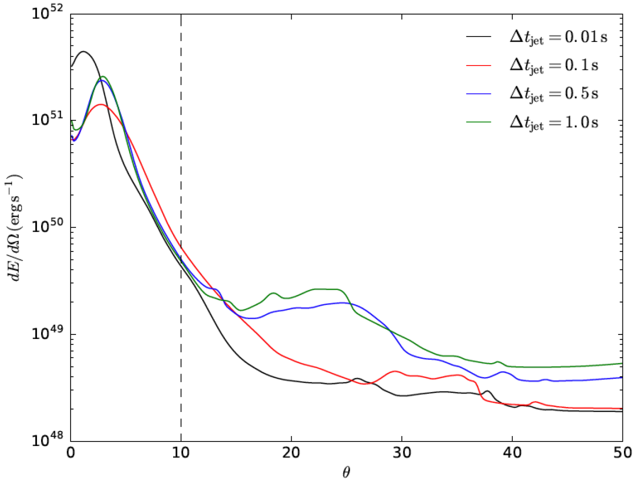

Depends on the waiting time for jet launching, current data cannot tell

Central engine (black hole vs. massive neutron star or magnetar)

GRB central engine

Hyper-Accreting Black Hole

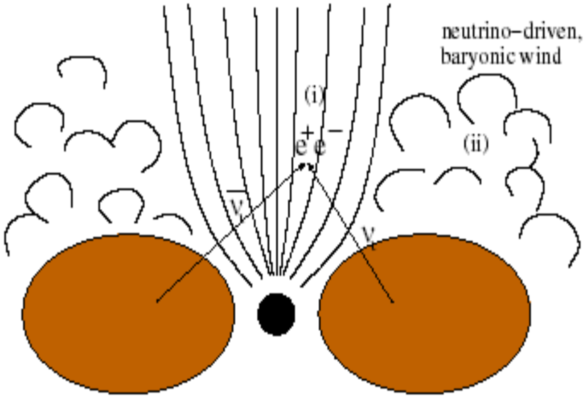

Neutrino annihilation

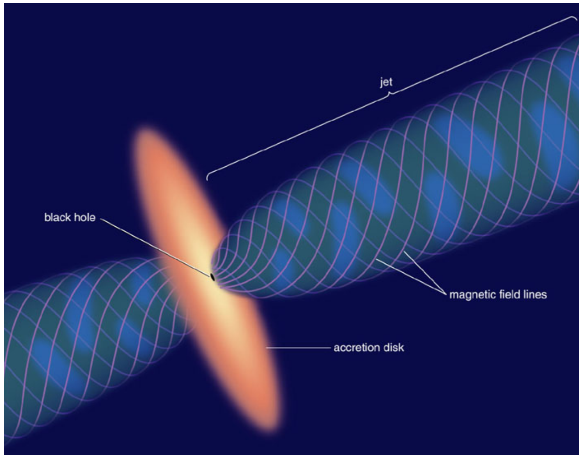

Magnetically tapping BH spin energy (Blandford-Znajek)

Millisecond Magnetar

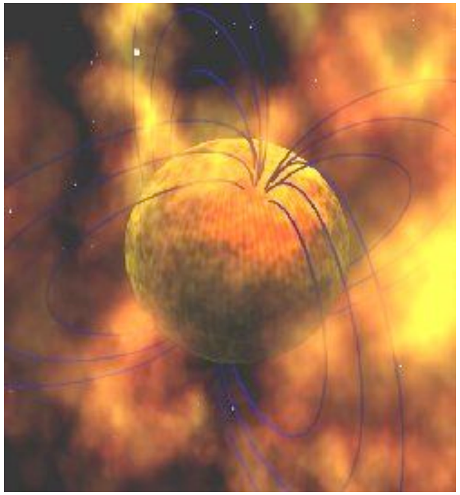

Likely both engines are operating in both types of GRBs

NS-NS merger products

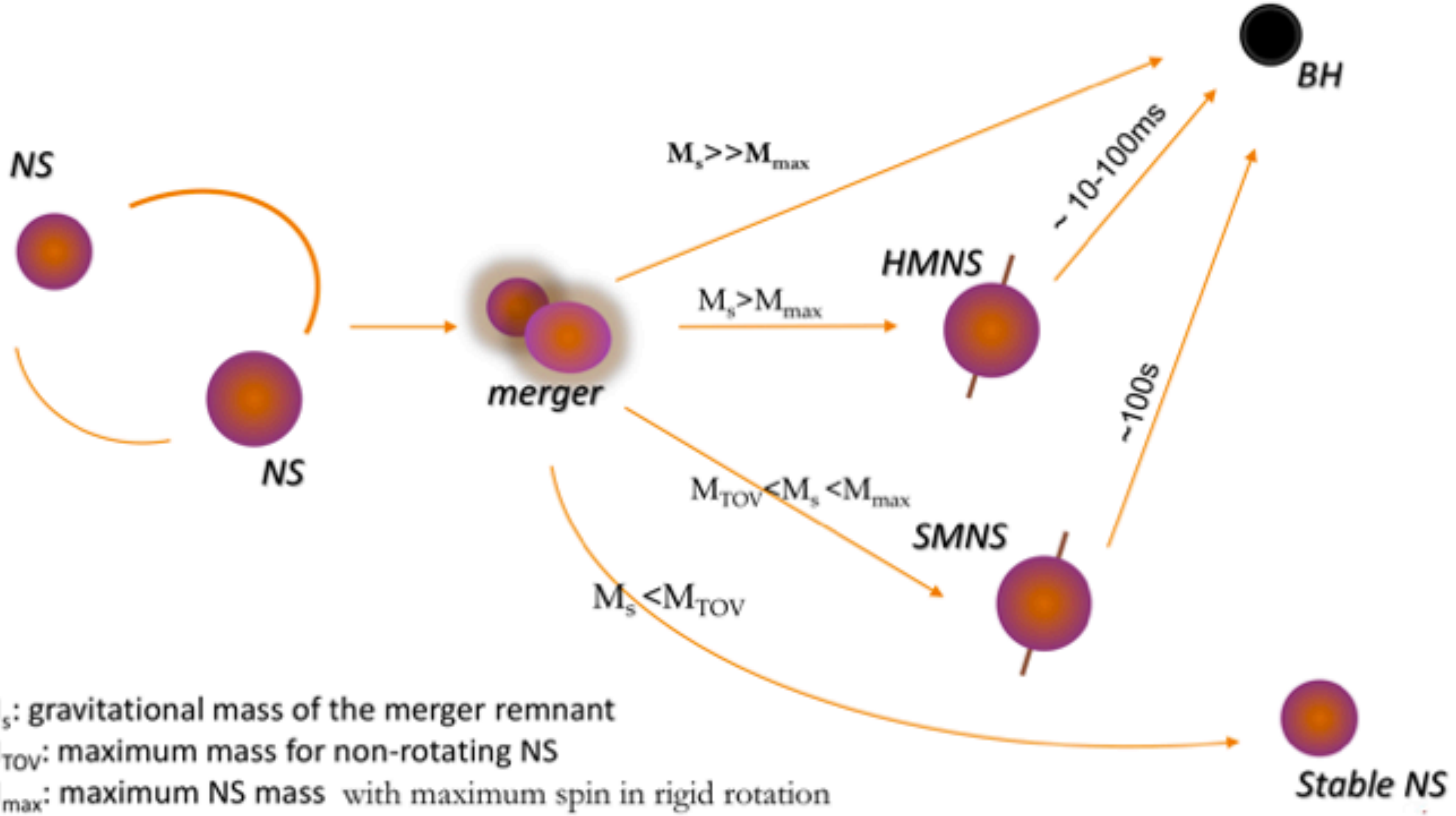

M_s: gravitational mass of the merger remnant
M_{TOV}: maximum mass for non-rotating NS
M_{max}: maximum NS mass with maximum spin in rigid rotation

Origin of the 1.7 s delay?

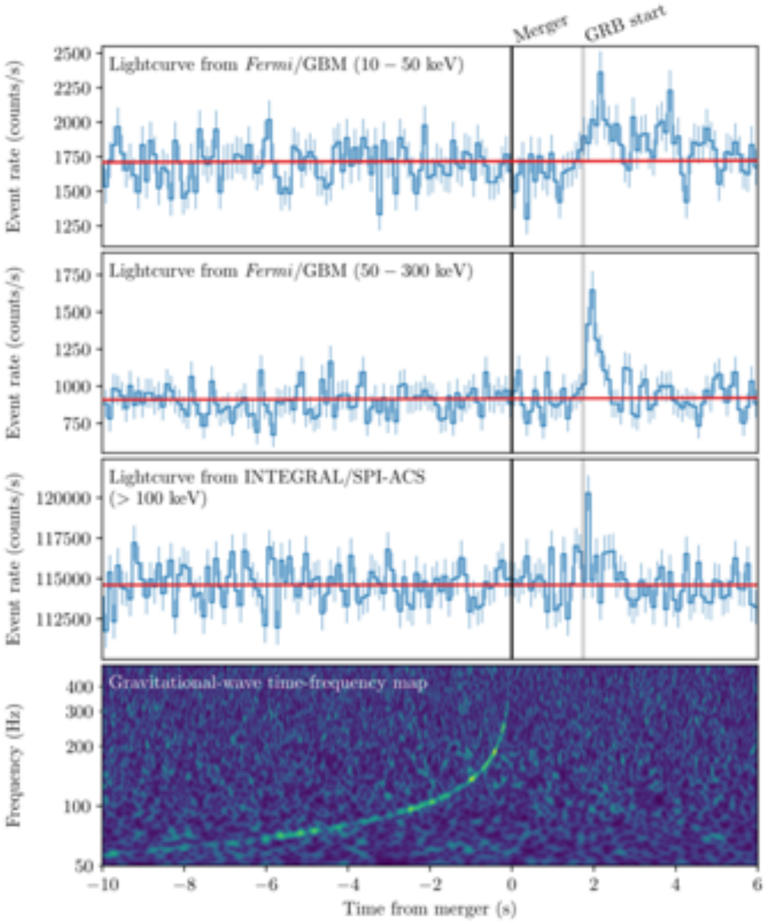

$$\Delta t = (\Delta t_{\rm jet} + \Delta t_{\rm bo} + \Delta t_{\rm GRB})(1+z),$$

waiting time for jet launching

jet breakout time

Time to reach GRB radius

$$\Delta t_{\rm GRB} \simeq (1-\beta\cos\theta)\frac{R_{\rm GRB}}{c} \simeq \frac{R_{\rm GRB}}{\Gamma^2 c}.$$

$$T_{\rm GRB} \sim \frac{R_{\rm GRB}}{\Gamma^2 c}.$$

$\sim$*2 s*

$\sim$*1.7 s*

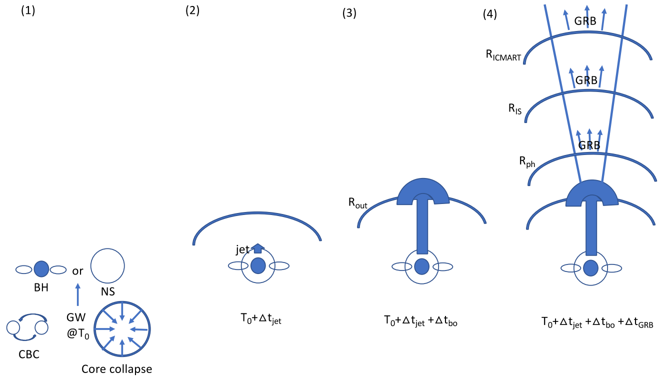

Delay time ~ duration
Not evidence of forming a BH

Zhang, 2019, Frontiers of Physics, arXiv:1905.00781

Summary

- The “big picture” of GRBs is “solved”.
- Several questions remain open:
  - Jet composition
  - Energy dissipation mechanisms
  - Radiation mechanisms
  - Central engine: black hole vs. magnetar
- There might not be one correct answer:

Everybody is correct (to some degree)!

All the models are probably relevant for some GRBs!

Back up slides

Millisecond magnetars in long GRBs

Lü & Zhang 2014, ApJ, 785, 74

- *750 Swift GRBs detected before Dec. 2013*
- *Gold sample (internal plateaus): 9 altogether, 3 with redshift*
- *Silver sample (external plateaus satisfying magnetar criteria): 69 altogether, 33 with redshift*
- *Aluminum sample (other external plateaus): 135 altogether, 67 with redshift*
- *Non-magnetars (no evidence): over 400, 111 with redshift*

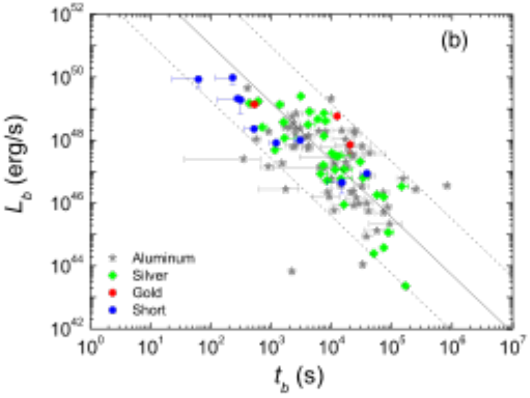

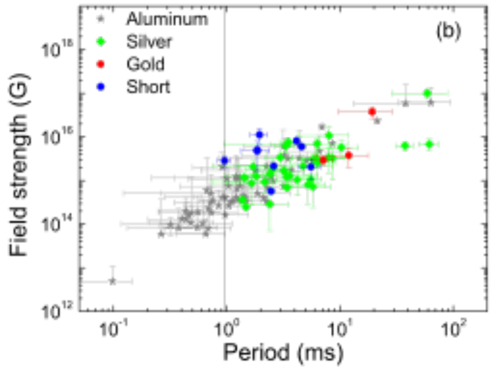

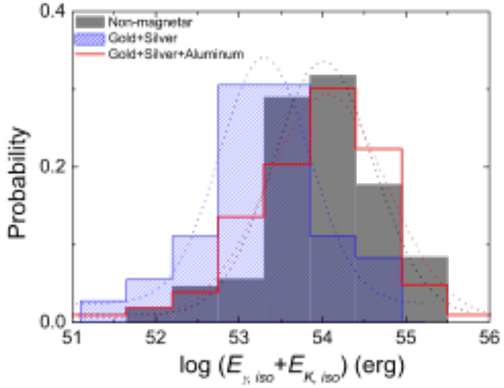

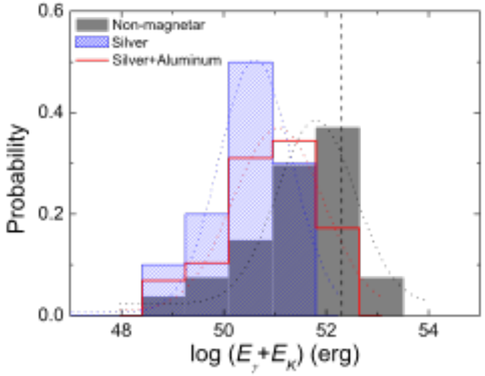

Millisecond magnetars in short GRBs

Lü et al. 2015, ApJ, 805, 89

- *40 Swift short GRBs or short GRBs with extended emission (EE), Jan. 05 – Aug. 14*
- *22 internal plateaus!*
- *10 external plateaus*
- *8 without plateau*

- *EE and internal plateaus are the same thing!*
- *The prevalence of the internal plateau likely a result of low medium density*

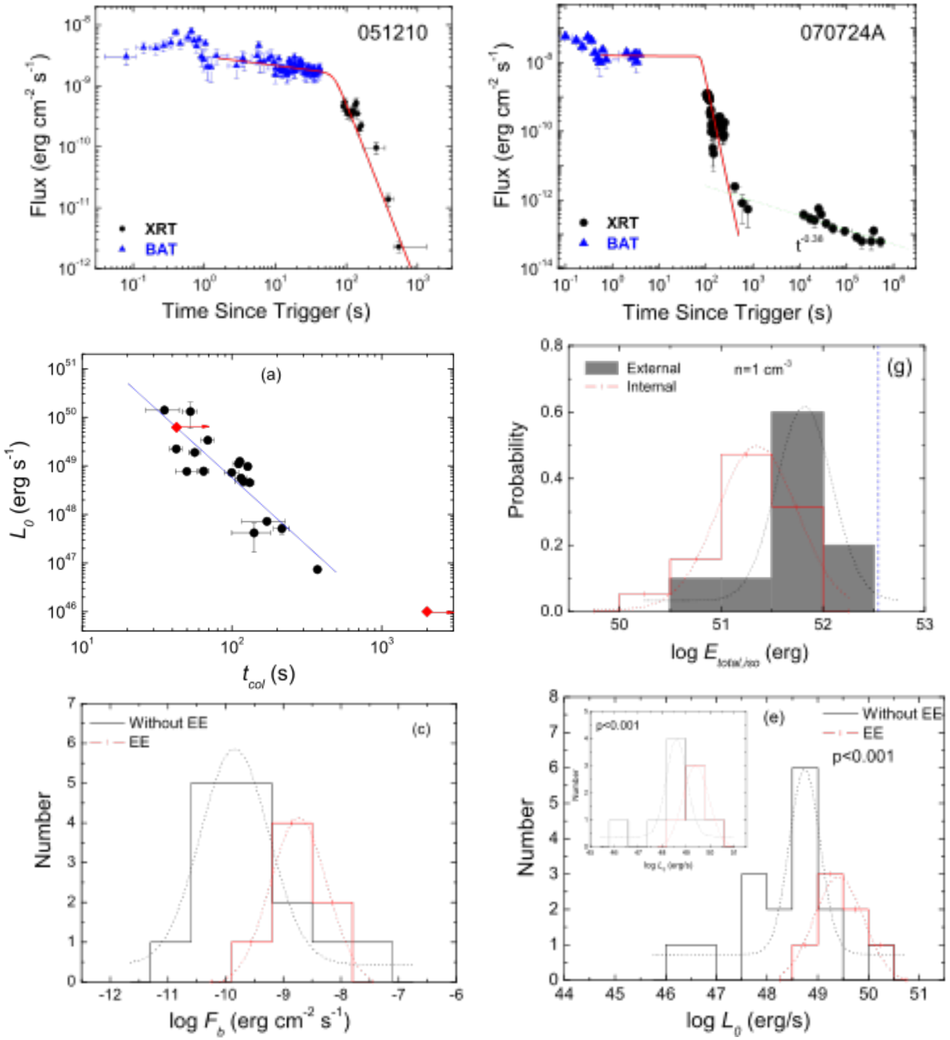

AT2017gfo:

Blue and red (and purple?)

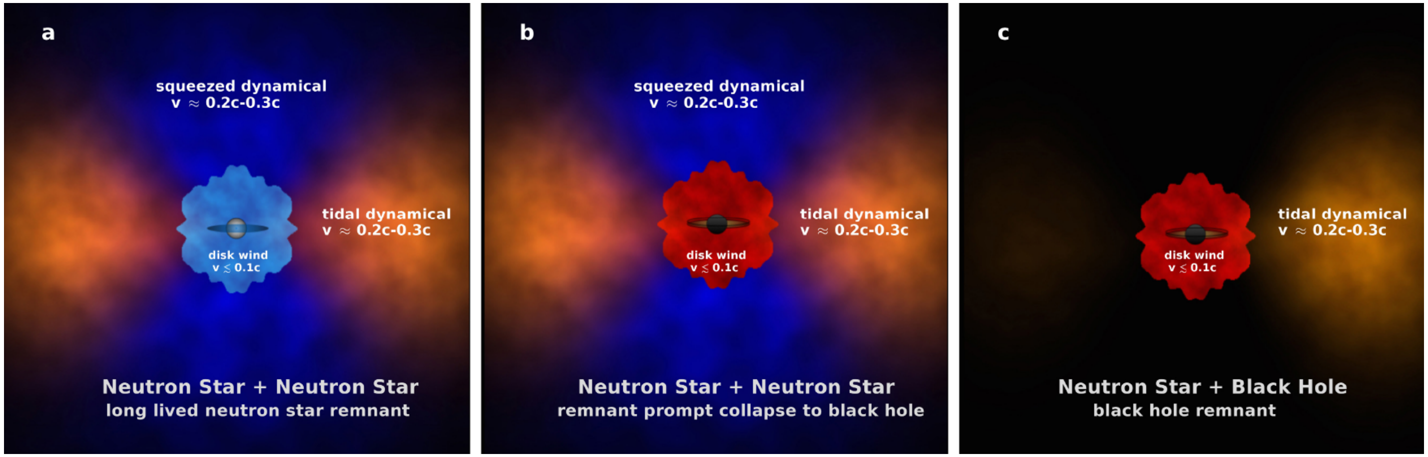

Kasen et al. 2017

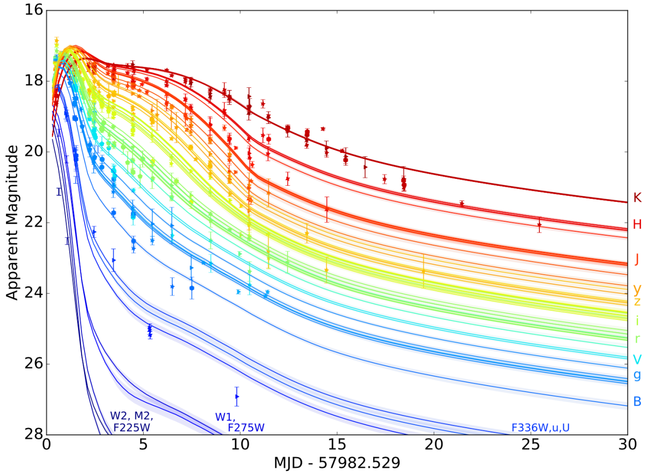

Villar et al. 2017

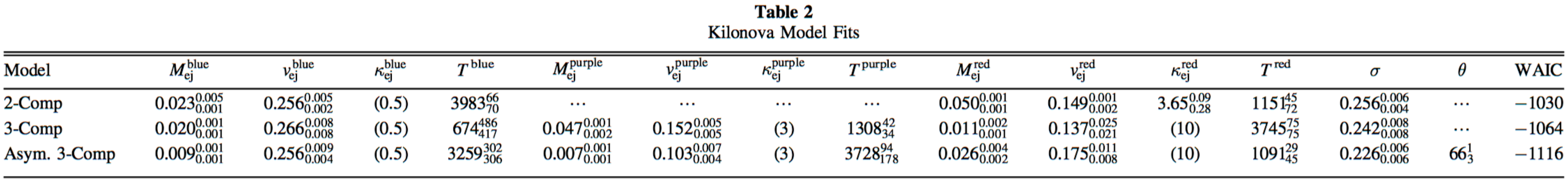

Table 2

Kilonova Model Fits

Model	$M_{\rm ej}^{\rm blue}$	$v_{\rm ej}^{\rm blue}$	$\kappa_{\rm ej}^{\rm blue}$	$T^{\rm blue}$	$M_{\rm ej}^{\rm purple}$	$v_{\rm ej}^{\rm purple}$	$\kappa_{\rm ej}^{\rm purple}$	$T^{\rm purple}$	$M_{\rm ej}^{\rm red}$	$v_{\rm ej}^{\rm red}$	$\kappa_{\rm ej}^{\rm red}$	$T^{\rm red}$	σ	θ	WAIC
2-Comp	$0.023^{0.005}_{0.001}$	$0.256^{0.005}_{0.002}$	(0.5)	3983^{66}_{70}	⋯	⋯	⋯	⋯	$0.050^{0.001}_{0.001}$	$0.149^{0.001}_{0.002}$	$3.65^{0.09}_{0.28}$	1151^{45}_{72}	$0.256^{0.006}_{0.004}$	⋯	−1030
3-Comp	$0.020^{0.001}_{0.001}$	$0.266^{0.008}_{0.008}$	(0.5)	674^{486}_{417}	$0.047^{0.001}_{0.002}$	$0.152^{0.005}_{0.005}$	(3)	1308^{42}_{34}	$0.011^{0.002}_{0.001}$	$0.137^{0.025}_{0.021}$	(10)	3745^{75}_{75}	$0.242^{0.008}_{0.008}$	⋯	−1064
Asym. 3-Comp	$0.009^{0.001}_{0.001}$	$0.256^{0.009}_{0.004}$	(0.5)	3259^{302}_{306}	$0.007^{0.001}_{0.001}$	$0.103^{0.007}_{0.004}$	(3)	3728^{94}_{178}	$0.026^{0.004}_{0.002}$	$0.175^{0.011}_{0.008}$	(10)	1091^{29}_{45}	$0.226^{0.006}_{0.006}$	66^{1}_{3}	−1116

AT2017gfo

$$t_p = \left(\frac{3M\kappa}{4\pi\beta v c}\right)^{1/2}$$

$$\approx 1.6\,\mathrm{d}\left(\frac{M}{0.01M_\odot}\right)^{1/2}\left(\frac{v}{0.1c}\right)^{-1/2}\left(\frac{\kappa}{1\,\mathrm{cm^2\,g^{-1}}}\right)^{1/2} \quad (3)$$

$$L_p = 1.2\times10^{41}\,\mathrm{erg\,s^{-1}}$$

$$\left(\frac{M}{0.01M_\odot}\right)^{1-\alpha/2}\left(\frac{v}{0.1c}\right)^{\alpha/2}\left(\frac{\kappa}{1\,\mathrm{cm^2\,g^{-1}}}\right)^{-\alpha/2} \quad (4)$$

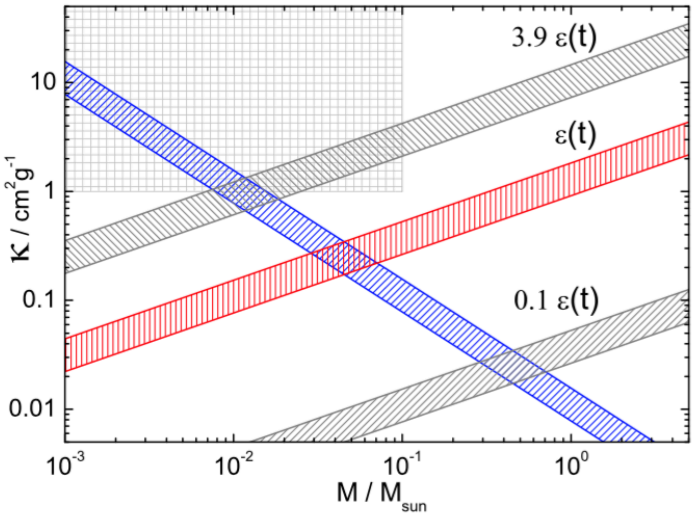

Li et al. 2018, ApJ, 861, L21

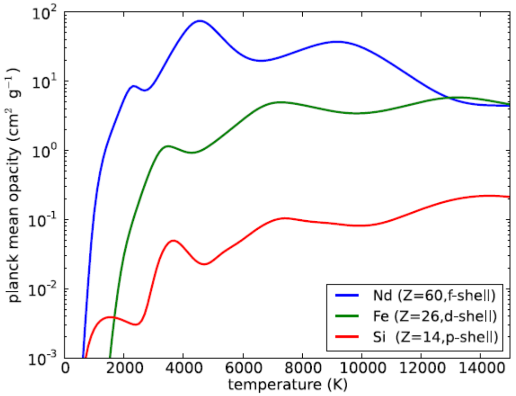

Figure 6. Planck mean expansion opacities for three different elements, showing the expected dependence on atomic complexity. The Nd opacities (blue line, $Z = 60$, open f-shell) were derived from `Autostructure` models, while the silicon (red line, $Z = 14$, open p-shell) and iron (green line, $Z = 26$, open d-shell) opacities used Kurucz line data. The calculations assume a density $\rho = 10^{-13}$ g cm^{-3} and a time since ejection $t_{\rm ej} = 1$ days.

(A color version of this figure is available in the online journal.)

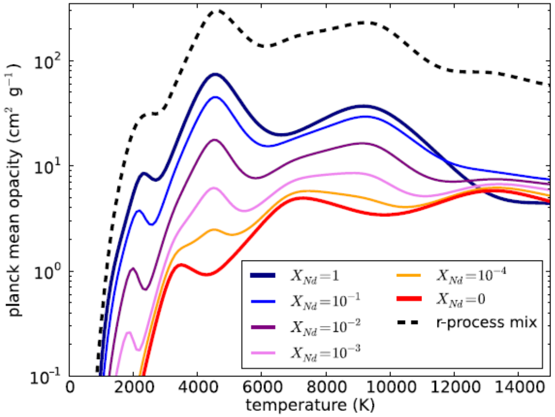

Figure 10. Dependence of the mean expansion opacity on the abundance of lanthanides. The solid lines show the Planck mean opacity for various mass fractions of neodymium in a mixture with iron. The dashed line shows the opacity of the approximate r-process mixture (with all 14 lanthanides) discussed in Section 6.

Kasen et al. 2013

AT2017gfo: long-lived-NS-driven?

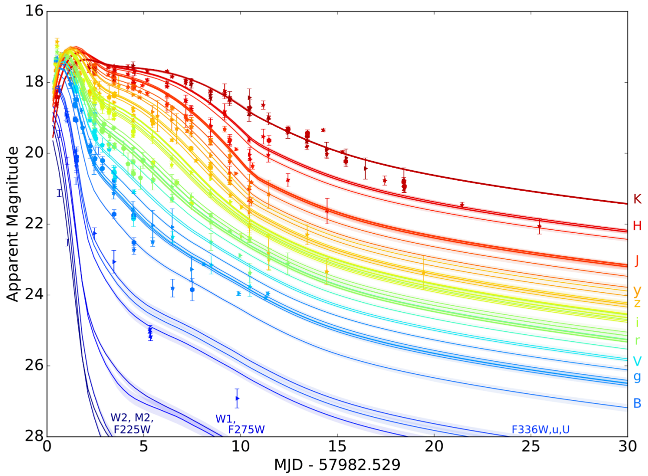

Villar et al. 2017

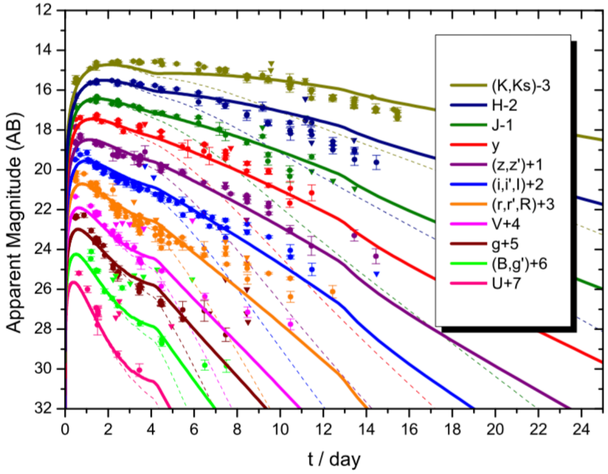

Yu, Liu & Dai, 2018, ApJ, 861, 114

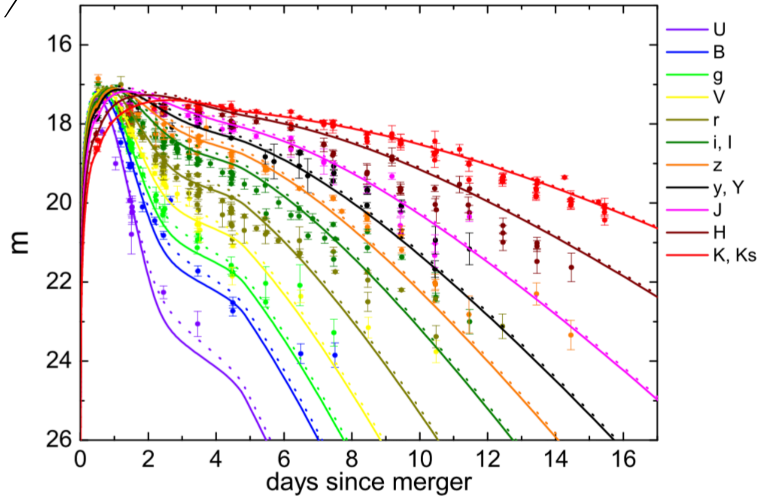

Li et al. 2018, ApJ, 861, L21

	$M_{\rm fb,i}/M_\odot {\rm s}^{-1}$	$L_{\rm md,i}/{\rm erg\,s}^{-1}$	$t_{\rm sd,gw}/{\rm s}$	B/G	ϵ	ejecta	$M_{\rm ej}/M_\odot$	$\kappa/{\rm cm}^2{\rm g}^{-1}$	$v_{\rm ej,i}/c$	Ω	δ	ζ	A
NS	-	3.4×10^{44}	500	3.4×10^{12}	0.0035	polar	1×10^{-3}	1	0.35	2π	-1	10	6
						equatorial	5×10^{-3}	5	0.2	2π	-1	10	6

GW170817:

Is a long-lived NS allowed?

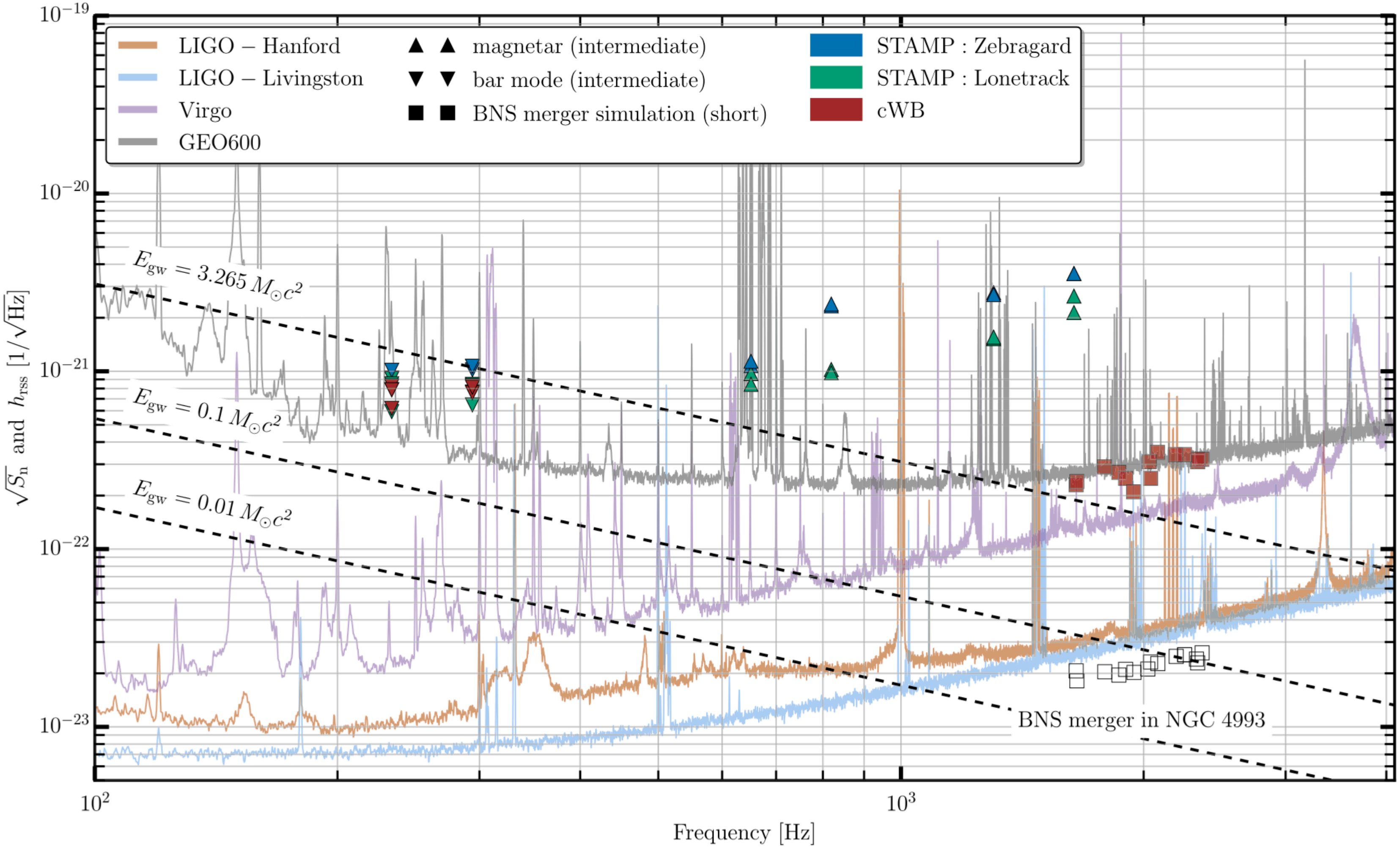

GW constraints: upper limit at least one order above prediction
Abbott et al. 2017, ApJL, 851, L16

GW170817:

Is a long-lived NS allowed?

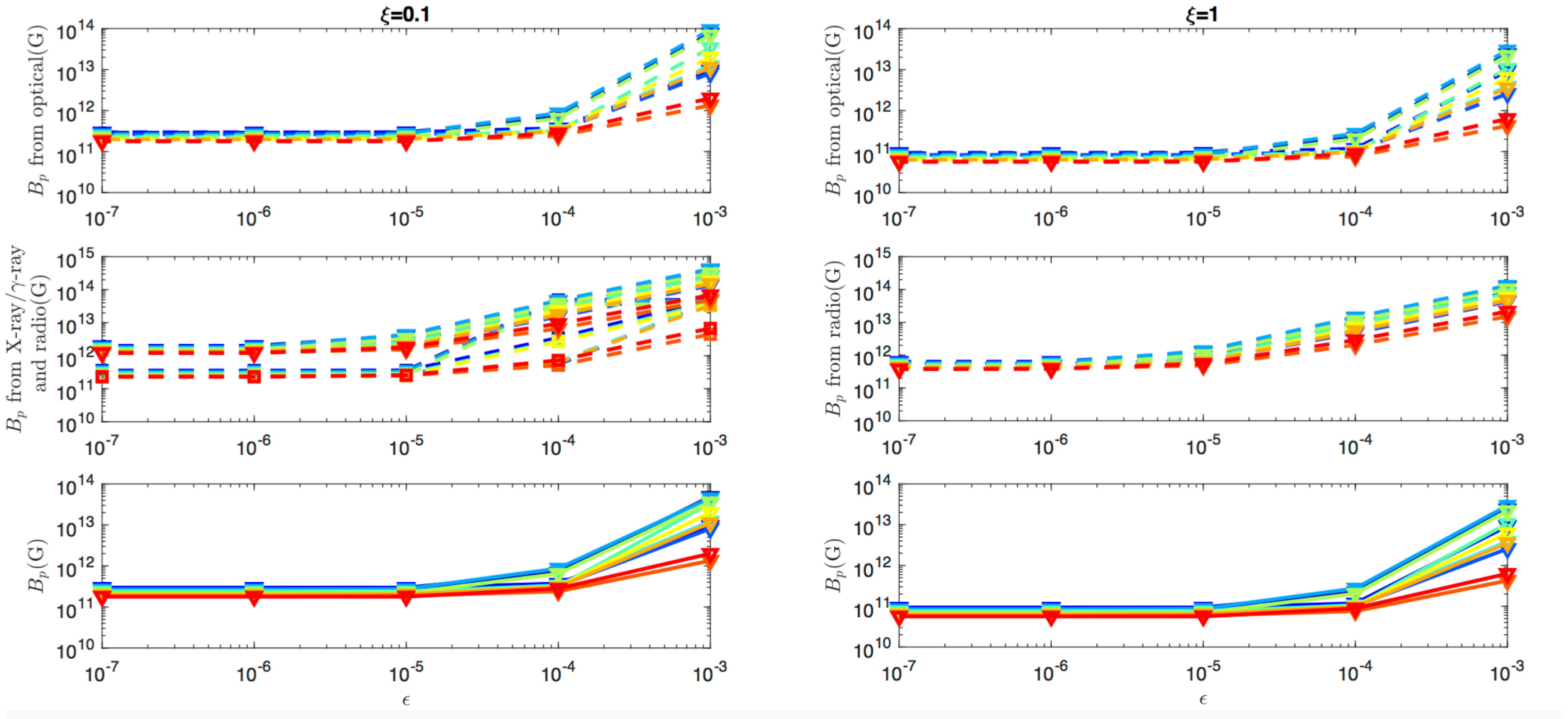

EM constraints: As long as Bp is low – constraints from UV/optical/IR (upper), gamma/X/radio (middle) and multi-band (lower)

Ai et al. 2018, ApJ, 860, 57

A late time X-ray “flare”?

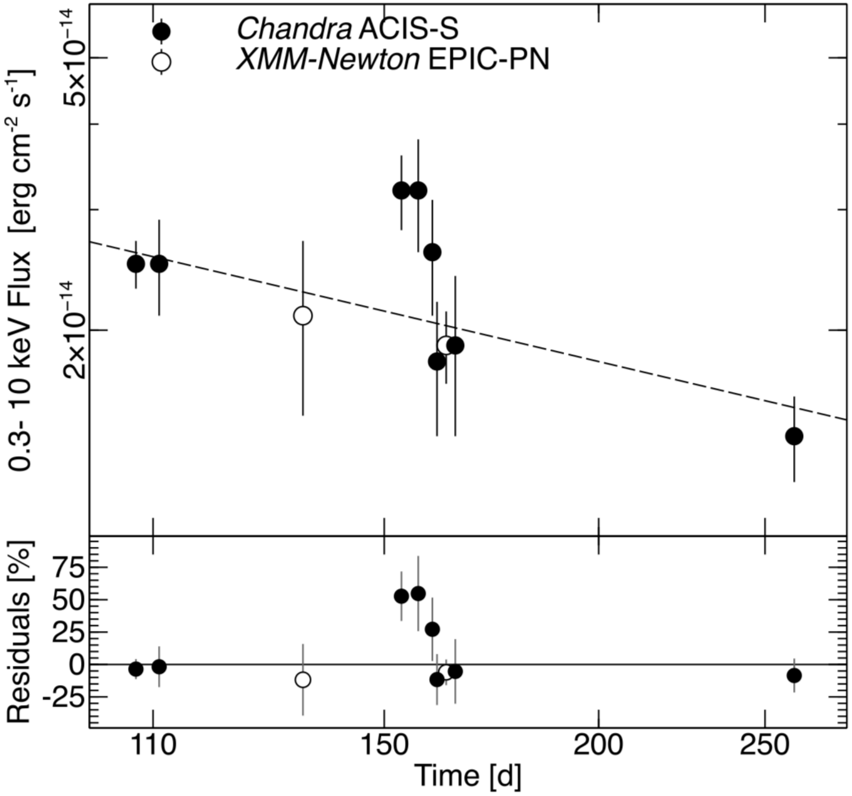

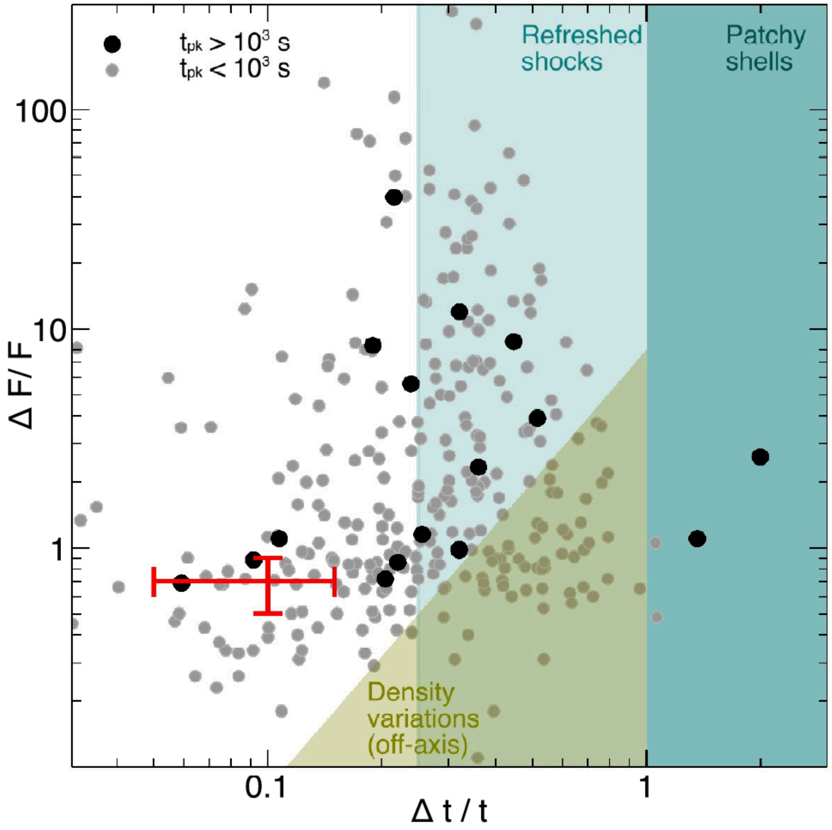

Piro, Troja, Zhang et al., 2019, MNRAS, 483, 1912